ABSTRACT

LUCERO, GABRIEL ANTONIO. Prompt Gamma Spectroscopic Analysis of Nuclear Fallout to Evaluate Sensitivity to Nuclear Device Characteristics. (Under the direction of John Mattingly).

In the event of a nuclear attack, timely and accurate identification of the device characteristics used in the detonation would be critical to national security. Traditional methods for forensic analysis of post-detonation debris, a.k.a., nuclear fallout, rely on wet chemistry to prepare samples for mass spectroscopic analysis. Sample preparation can potentially delay the analysis by days to weeks during which time many short-lived fission products will decay away. However, gamma spectroscopy can be performed in the field as soon as investigators arrive on site and collect fallout samples. This thesis demonstrates that some nuclear device characteristics can be identified by analyzing the gamma spectrum of nuclear fallout 3 to 18 days after detonation. The Defense Land Fallout Interpretive Code (DELFIC) was used to simulate hundreds of nuclear detonations while varying device characteristics, atmospheric conditions at the time of detonation, and gamma spectrum observation conditions (sample location, fallout particle diameter, and fallout collection time after detonation). This thesis also demonstrates that the variance in the fallout gamma spectrum caused by physical fractionation can be virtually eliminated by controlling fallout particle diameter to a narrow range. Finally, this thesis applies rigorous statistical analysis to identify several gamma spectrum photopeaks that can be used to categorize the fissile material contained in the device and the spectrum of neutrons inducing fission during device detonation.

Prompt Gamma Spectroscopic Analysis of Nuclear Fallout to Evaluate Sensitivity to Nuclear Device Characteristics

by
Gabriel Antonio Lucero

A thesis submitted to the Graduate Faculty of
North Carolina State University
in partial fulfillment of the
requirements for the degree of
Master of Science

Nuclear Engineering

Raleigh, North Carolina

2016

APPROVED BY:

_____	_____
Brandon Grogan	Joseph Guinness

_____
John Mattingly (Committee Chair)

DEDICATION

To my family, especially my wife Natalia. I would not be here without you.

BIOGRAPHY

Gabriel Lucero was born on 14 November, 1983. He grew up in Las Vegas, NM. After finishing high school he attended the United States Military Academy at West Point from 2002-2006 where he majored in Nuclear Engineering. Upon graduation from the Academy he was commissioned a Second Lieutenant of Aviation in the United States Army. He has served in several assignments including 2 tours to Afghanistan. He was admitted to North Carolina State University's Nuclear Engineering Department in 2012 while still on active duty. Following his graduation from NCSU he will be assigned to the Physics and Nuclear Engineering Department at West Point. He is married to the former Natalia Mendoza. They have two daughters, Sofia and Sienna.

ACKNOWLEDGMENTS

I would like to sincerely thank my advisor Dr. John Mattingly. It has been a pleasure working with you. Your passion for research was contagious. The professionalism you displayed as an advisor, educator, and mentor are traits I aspire to. I would also like to thank my committee members, Dr. Guinness and Dr. Grogan, for their thoughtful feedback. I would like to thank Dr. Vincent Jodoin, Dr. David Hooper, and the team at Oak Ridge for their training and prompt assistance with any issue that I encountered during my research. Finally I would like to thanks my research group for all your help and support.

TABLE OF CONTENTS

LIST OF TABLES

LIST OF FIGURES

1 Introduction

1.1 Motivation/Background

In his 2015 National Security Strategy, President Barack Obama states, “No threat poses as grave a danger to our security and well-being as the potential use of nuclear weapons and materials by irresponsible states or terrorists” [1]. The statement highlights the danger imposed by the potential use of nuclear weapons on domestic soil. The motivation of this thesis is to use gamma spectroscopy to advance the field of nuclear forensics. Specifically this thesis demonstrates the application of rigorous statistical analysis to identify gamma spectroscopic features that can be used to characterize a nuclear device by the composition of the fallout. This includes examining the effects of fractionation. Fractionation is the process by which the various fallout particles leave the initial mushroom cloud through chemical or physical processes; it determines the specific radionuclide composition of the fallout at a given location relative to ground zero. The primary objectives of this research are to:

- Examine the effect of controlling fallout particle size on the nuclear fallout gamma spectrum
- Demonstrate that variance due to physical fractionation can be virtually eliminated by controlling particle size.
- Test the robustness of this effect by analyzing hundreds of nuclear simulations while varying device characteristics and observation conditions (gamma ray energy, sample location, fallout particle diameter, fallout collection time after detonation)
- Use statistical modeling and hypothesis testing to make statements of significance about the variance associated with different nuclear detonation simulation input parameters
- Provide a list of radionuclides that are most sensitive to nuclear fuel material used to create the device and/or neutron energy spectrum used to induce fission in the device

If a nuclear device was deployed against the citizens of the United States or our allies, one of the primary concerns, after caring for the injured, would be to determine the parties responsible for this act. In today's complex international political environment, the list of possible suspects makes identification of responsible parties difficult. Similar to criminal forensics, nuclear forensics deals with the analysis of post detonation evidence in an attempt to assess culpability. Questions of interest include:

- If the weapon used Highly Enriched Uranium (HEU), then what was the enrichment of the HEU?
- If the weapon used plutonium, how long was the source of uranium irradiated in a reactor to make the plutonium?
- How long since the plutonium was last purified?
- What level of sophistication was used to make the device?
- Was the device a pure fission weapon or were fusion reactions used to increase the explosive yield [2]?

These characteristics would prove useful in identifying the origin of the device. The area of nuclear forensics explored in this thesis is the gamma spectrum analysis of nuclear fallout particles using computer simulations. Current analysis techniques employ mass spectrometry which involves chemically and physically separating the particles in laboratories, a process that can take on the order of weeks [2]. Gamma spectroscopy can be used to measure fallout particles directly and analysis can be conducted in the field as soon as investigators arrive on-site and collect fallout samples. The time frame for making determinations about device characteristics using gamma spectroscopy would be on the order of days as opposed to weeks. In addition, the presence of short lived fission products could be used to enhance the analysis prior to decaying away. This would be a significant advantage as it would provide policymakers with a fuller picture of the event to inform a responsible national response.

Since the adoption of the Comprehensive Test Ban Treaty, it has not been possible to measure the gamma spectrum of nuclear fallout using state of the art gamma spectrometers. However, computer codes that simulate nuclear detonations were developed in the 1960's and 1970's and have been steadily improving. Computing speeds and advances in cluster computing have also been steadily improving. These advances make simulation analysis a viable option for studying nuclear forensics. The simulation code used in this work is the Defense Land Fallout Interpretive Code (DELFIC.) The current version of DELFIC has been maintained and developed by the Oak Ridge National Laboratory Nuclear Security Modeling Group. This version has several updates and features that make it useful for modeling nuclear detonations and the subsequent fallout that is produced by the initial explosion [3]. This includes:

- Modeling the abundance of fallout particles produced by various types of nuclear explosions
- Modeling the radionuclides contained in the particles
- Simulating the dispersion of fallout particles on the ground while factoring in meteorological conditions at the time of detonation

The prospect of having to conduct nuclear forensics in a real world scenario may hopefully never have to be used, but any research that would better prepare collection and analysis teams to perform their duties would be advantageous to our national security. This motivated the research.

1.2 Prior Work

Some of the first work done in post-detonation nuclear fallout was performed in the 1960's. Heft examined the radionuclide composition of nuclear fallout, testing its dependence on particle size by examining the air filter sample placed around nuclear test detonations [4]. Heft found that indeed the distribution of certain radionuclides in fallout particles was dependent on

particle diameter. He was able to characterize the distribution of radionuclides in fallout for land, surface, and subsurface burst. He did this by examining the fallout produced by differing soil compositions and meteorological conditions. One important conclusion from the work was that it is possible to relate the fractionation behavior of all radionuclides by comparing a single pair of volatile/refectory radionuclides. Volatile radionuclides are distributed on the surface of fallout particles, while refractory radionuclides are distributed throughout the volume of the fallout particle. This was some of the first work which attempted to characterize the fractionation effect by comparing volatile and refractory radionuclides. Early work conducted on the subject is especially useful because analyses of actual nuclear tests were used, and results from current simulations can be benchmarked by comparing the results.

Freiling also examined post-detonation fallout. He did not examine post-detonation fallout for the purposes of nuclear forensics but instead he wanted to accurately model the composition of fallout particles in order to predict the fallout field contamination and radiological exposure. His work further examined the effects of fractionation [5]. Freiling was also able study fallout from multiple nuclear tests. Through his study of nuclear detonations in various conditions (multiple soil types, explosive yields, and meteorological conditions, etc.), he found that the presence of most radionuclides measured in fallout was insensitive to changing environmental conditions. From this he concluded that the radionuclides present in fallout were primarily dependent on the device characteristics themselves.

Freiling also examined the dependence between radionuclide composition of fallout particles and fallout particle diameter [6]. He examined three particle diameter groups, or what he called local, intermediate, and worldwide fallout. He observed logarithmic correlations between the degree of fractionation and particle size. From this correlation he presented a means to estimate the degree of fractionation occurring in all fallout particles. He then used the degree of fractionation to estimate the unique radioactivity present in each of the three particle sizes. The work characterized the degree of fractionation present in fallout by presenting the abundance of all mass chains as a ratio of a purely refractory mass chain. A mass chain is a group of

radionuclides that undergo beta decay to convert a neutron to a proton or vice versa. Mass number is conserved in the decay, hence the name mass chain. This resulted in a more accurate prediction of the radionuclide composition. When the radionuclide composition was combined with the distribution of particles in a nuclear fallout field, his results showed a more accurate way to estimate exposure rates.

More recently, short-lived fission products have been examined by Miley et al. to monitor compliance with the Comprehensive Nuclear Test Ban Treaty [7]. Their team conducted gamma spectroscopic analysis of air filters to provide positive proof of an atmospheric explosion. The results included a list of radionuclides that were useful in identifying nuclear detonations. This paper included two experiments: one experiment replicating field detection by the International Monitoring System (IMS), and another experiment replicating laboratory analysis of samples that would be transported to various laboratories after initial detection. The samples used in both tests were created in a research reactor thermal port and replicated historical samples collected in Richland, WA from a low yield (~20 kt) nuclear test conducted at Lop Nor, China. To simulate IMS detection, samples were irradiated then allowed to decay for 12 days to account for atmospheric transport. For the experiment replicating laboratory analysis, samples decayed 4 additional days to replicate sample collection and shipment to laboratories. The experiment gave good insight into detectable gamma lines present in nuclear fallout a short time after detonation. A limitation in the experiment was that only fallout particles small enough to travel hundreds of kilometers were measured (as would be detected by IMS). Also, irradiated samples did not undergo the same chemical fractionation process that fallout particles formed in a nuclear blast would experience.

Experiments have also been performed to identify gamma line energies sensitive to fissile material and neutron energy by Marrs et al. Samples of ^{239}Pu, ^{235}U, and ^{238}U were irradiated with a neutron beam. Two neutron energies were used in the experiment, thermal neutrons and 14-MeV neutrons. Each fuel sample underwent approximately 10^8 fissions. High purity germanium detectors were then used to measure the gamma spectrum of the sample from 1 minute to 14

hours after irradiation [8]. The results showed multiple gamma lines that were sensitive to fuel material and neutron energy. One important result was that all the significant mass chains identified in the experiment originated from volatile mass chains.

Work has also been done using simulations and models. Miller used DELFIC to identify gamma peak ratios that are useful for determining the fissile material of the nuclear device [9]. Miller's work primarily focused on un-fractionated and refractory samples of nuclear fallout. The useful radionuclides identified were presented as ratios of purely refractory radionuclides to reduce sample size variation and to fix chemical fractionation. Miller also performed a comprehensive analysis of soil solidification times and particle size modeling in DELFIC. His work illustrated how DELFIC models the fractionation changes of fallout as a function of particle radius and soil solidification time.

Smith also did research on identifying device characteristics using gamma spectroscopy from DELFIC simulations coupled to the Gamma Detector Response and Analysis Software (GADRAS), which simulates the detector response of multiple commercial gamma ray detectors. Smith was able to identify gamma ray peak energy ratios that are useful in identifying fissile material and neutron energy of a nuclear device between 6 and 48 hours after detonation [10]. Her work focused on determining device characteristic even if explosive yield was not immediately known. The primary technique used was to identify mass chains sensitive to fuel type and fission yield and compare them to mass chains that are insensitive to fuel type and fission yield.

1.3 Novel Contributions

This thesis makes several novel contributions to application of gamma spectroscopy for the analysis of nuclear fallout:

- This thesis utilizes a code to optimize DELFIC sample location based on minimum dose received on-site and maximum desired density of fallout on the ground. This implementation of DELFIC would assist collection teams in route planning.

- Also implemented was a scalable code suite that runs hundreds of DELFIC simulations. The results are then combined into a single data file that can then be analyzed by the user.
- DELFIC was used to determine gamma spectrum sensitivity to various nuclear fallout input parameters while controlling fallout particle size.
- Statistical analysis was applied to the results by using linear regression and the F-Test to make statements of significance about nuclear device input variables.

2 Modeling Nuclear Fallout Production, Transport, and Deposition

The formation of post-detonation fallout is a complex process. Many factors determine the final composition and location of the fallout particles. The two primary details of nuclear fallout theory that will be discussed in this chapter are how radionuclides are formed from the fission process, and how the fallout particles that constitute them are formed. Each section will cover the theory and the modeling tools used in the simulations.

The DELFIC [11], and the Oak Ridge Isotope Generation and Depletion Code (ORIGEN-S), were the two primary computer codes used in the simulations. DELFIC is a fallout prediction code first developed by the Defense Nuclear Agency in the 1960's. Various agencies have worked on the code since its original development, and the version of DELFIC used in this thesis is the version updated by ORNL in 2008. DELFIC models the formation of nuclear fallout in three main modules:

- Initialization and Cloud Rise Module (ICRM)
- Diffusive Transport Module (DTM)
- Output Processor Module (OPM)

The ICRM takes the user specified inputs and models the detonation through the rise and stabilization of the nuclear cloud, including the modeling of all the radionuclides and fallout particles initially created by the blast. The DTM transports the fallout from the stabilized cloud to the ground. The OPM processes the deposited fallout in informative maps of differing fallout characteristics (dose rate, fallout mass, time of onset of fallout, etc.) [12].

The final radionuclide composition and gamma emission of the fallout is modeled using ORIGEN-S. ORIGEN-S was developed by Oak Ridge National Laboratories to perform point depletion and decay analyses to obtain radionuclide concentrations, decay heat source terms, and

radiation source spectra [14]. The component of ORIGEN-S used in this thesis was the decay database. We used it to construct fallout gamma spectra given the radionuclide composition predicted by DELFIC.

2.1 Modeling Nuclear Fission Products

This section will give a general overview of the physical phenomena that create fission products and what equations are used to model the fission products. In the early stages of nuclear detonation, neutrons induce fission in the fuel material. The result is a rapid release of energy, ~200 MeV per fission 2; sometimes 3, lower mass number nuclei called fission "daughter" products; and neutrons [14] (other sub atomic particles and radiation are also released but they are not relevant to this thesis). These neutrons induce additional fissions of the fuel material and result in a runaway nuclear chain reaction in a nuclear detonation.

The production of fission products from neutron-induced fission constitutes a probabilistic event that has been studied and documented by numerous researchers. The yield probability tables used for this paper are drawn from the Evaluated Nuclear Data File B-VII.1 (data file used by ORIGEN-S) produced by Los Alamos National Laboratory, and the International Atomic Energy Agency's (IAEA) Handbook of Nuclear Data. [15] [16] The yield probability of daughter products is often plotted as a function of daughter product mass number, which is referred to as the "mass yield curve."

Figure 2-1 shows a mass yield curve. This figure comes from the fission of ^{235}U irradiated by fission spectrum neutrons. Some features to note on the figure are the two highest points which are referred to as "peaks," the "U" shape in the center or "saddle," and the edges along each peak. The peaks are the result of asymmetric fission where a light and heavy daughter product is produced. The saddle region is a result of nearly symmetric fission where the daughter products have almost the same mass number. The mass yield curve can be combined with the total numbers of fissions caused by a nuclear detonation to determine the mass chain abundance of daughter products. The fuel material used and neutron flux are specified for the figure because the mass yield curve changes as a function of both those parameters.

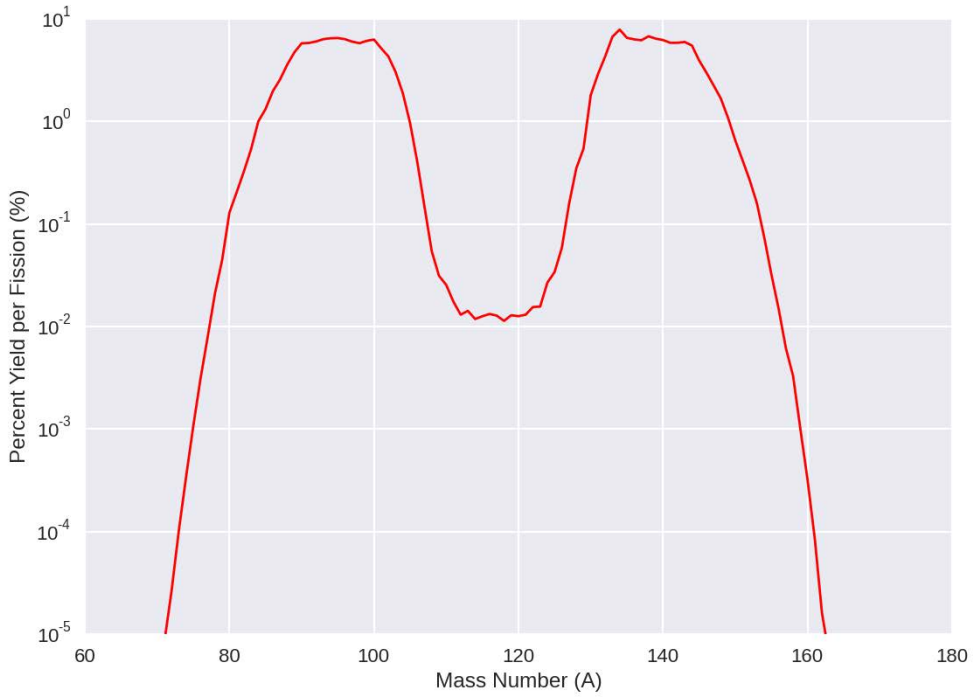

Figure 2-1 Mass yield curve of fission products from ^{235}U irradiated by fission spectrum neutrons

The qualitative radionuclide inventory of daughter products produced after a nuclear detonation is almost exclusively dependent on:

1. Fuel material used in the device (e.g., ^{235}U or ^{239}Pu)
2. The energy of the neutrons that were used to induce fission of the device (neutron flux)
3. Neutron capture by other materials (soil, buildings, inert bomb material etc.) [17]

2.1.1 Neutron Energy

The neutron energy used to induce fission in a nuclear device is divided into two categories, prompt fission neutrons and fusion neutrons. Nuclear detonations cannot be achieved with slow neutrons. [14] Prompt fission neutrons are those that originate from previous nuclear fissions. They are "born" with a continuous energy spectrum and have a mean energy of ~2 MeV. Figure 2-2 shows the distribution of neutron energies born from ^{239}Pu and ^{235}U induced fission. The distribution of energies is modeled using the Watt fission spectrum. The second category of neutron is fusion neutrons. For certain types of nuclear devices, neutrons produced by fusion reactions are used to subsequently induce fission. These neutrons originate from the fusion of deuterium and tritium (D-T reaction). The D-T reaction produces a mono-energetic neutron with energy of 14.1 MeV.

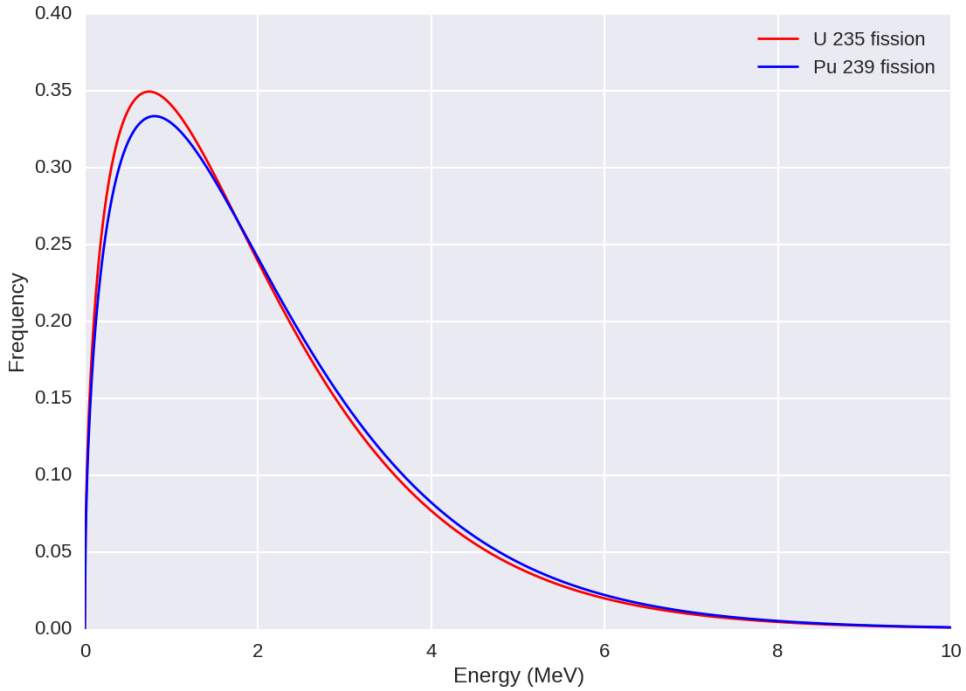

Figure 2-2 Watt prompt fission neutron spectrum ^{239}Pu and ^{235}U

Figure 2-3 shows the mass yield of fission daughter products produced by neutrons of different energies. We can see that the saddle region of the curve of is much shallower for the fusion energy neutrons. This happens because induced fission becomes more symmetric as the neutron energy increases. The plot is on a log-y scale so daughter products in the saddle region are produced with approximately 2 orders of magnitude difference between the two neutron energies. As a result, any nuclear devices detonated using fusion energy neutrons would have a much greater amount of daughter products located in the saddle region compared to similar nuclear devices that used fast fission neutrons to induce fission.

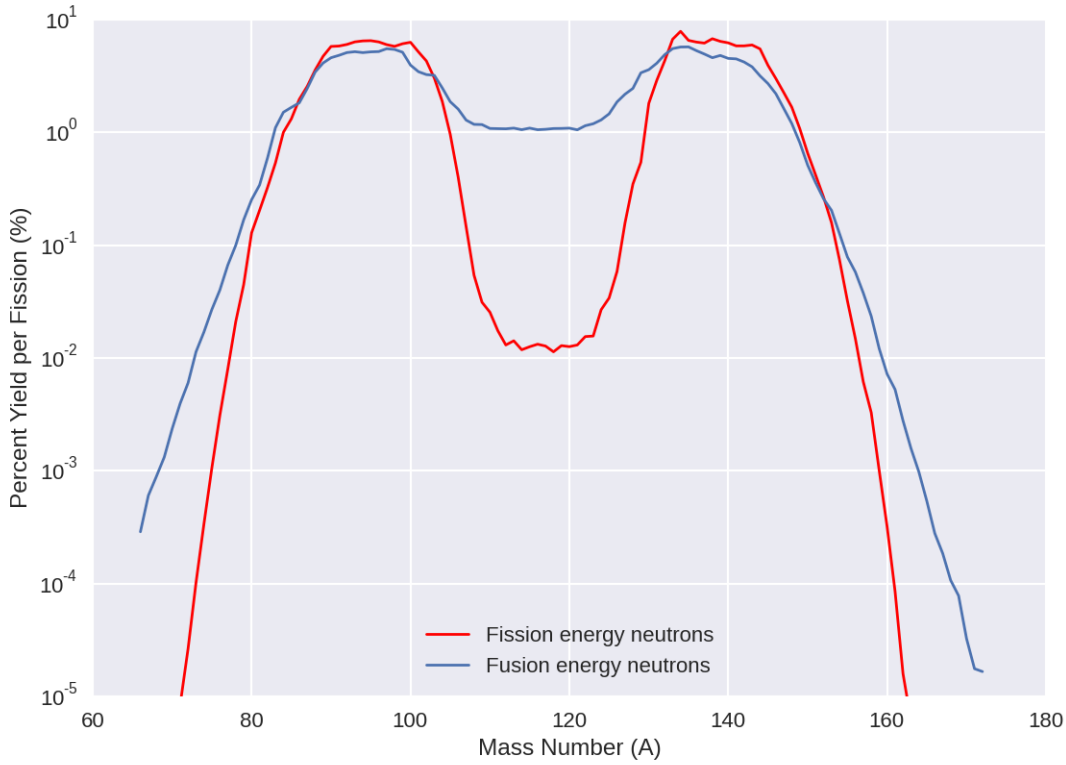

Figure 2-3 Mass yield curves of fission daughter products induced by neutrons of different energies in ^{235}U fuel

2.1.2 Fissile Material

Figure 2-4 shows how the shape of the mass yield curve changes as a function of different fuel material types. Here we can see that the curves are similar in shape, however there is a "shift" to the left and right between the differing fuel types. The reason for the shift is the difference in mass numbers between the fuel materials. ^{239}Pu has the highest mass number and as a result its mass yield curve is located to the right of ^{238}U and ^{235}U. Whereas the saddle of the mass yield curve was the distinguishing feature for nuclear devices made with differing incident neutron energy, the edges of the mass yield curve are the distinguishing features for nuclear devices made from differing fuel material types.

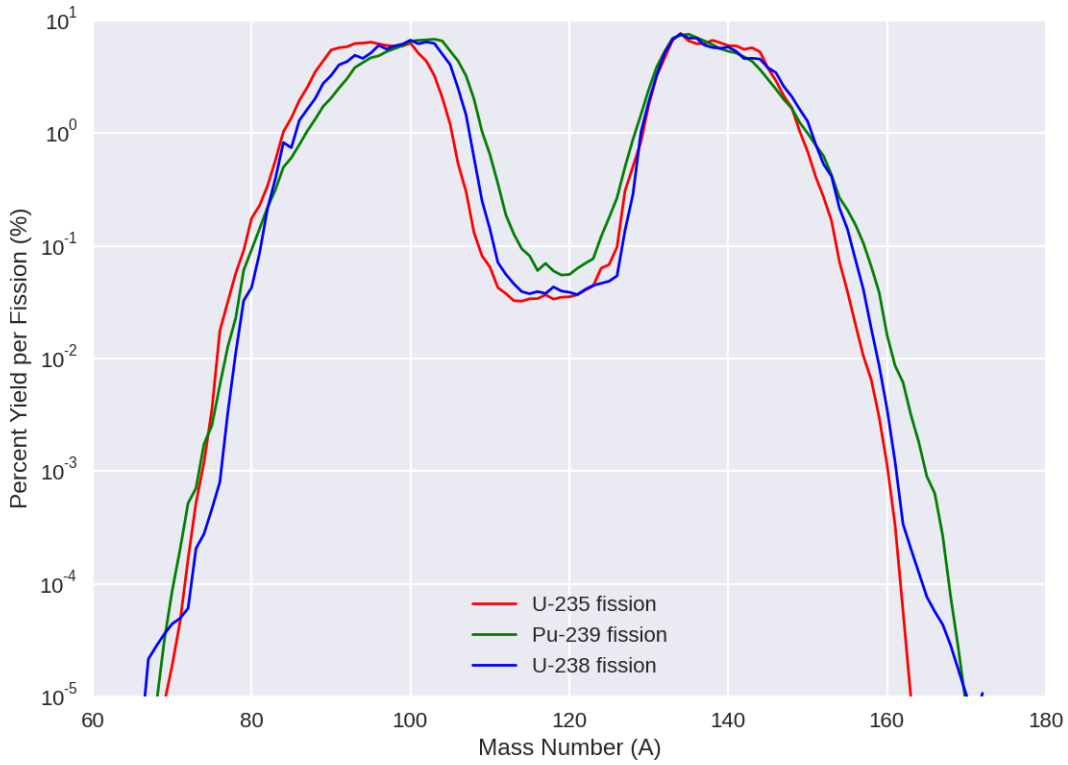

Figure 2-4 Mass yield of fission daughter products produced from different fuel type: ^{235}U, ^{238}U, and ^{239}Pu

2.1.3 Radioactive Decay

What should be noted from the previous mass yield curves is that they represent the distribution of the fission products immediately following a fission event. To determine the fission products present at a later time, the decay of daughter products must be calculated. The daughter products produced immediately following a nuclear detonation are often highly unstable due to an excess of neutrons in the nucleus. The radionuclide then transmutes to a more favorable neutron to proton ratio by undergoing nuclear decay. The predominant decay method of fission daughter products is beta-minus (β^-) decay. Equation (2.1) illustrates the equation for beta-minus decay. Here the nucleus converts a neutron to a proton by releasing a beta-minus particle and an anti-neutrino.

$$ {}^{A}_{Z}X \rightarrow {}^{A}_{Z+1}Y + \beta^- + \bar{\nu} \tag{2.1} $$

Following the beta-minus decay, the nucleus is often left in an excited state. It then relaxes to a more stable state by emitting gamma radiation. The relaxation and emission of gamma radiation happens on the order of picoseconds for a vast majority of radionuclides and is considered instantaneous when compared to the half-life of the beta-minus decay.

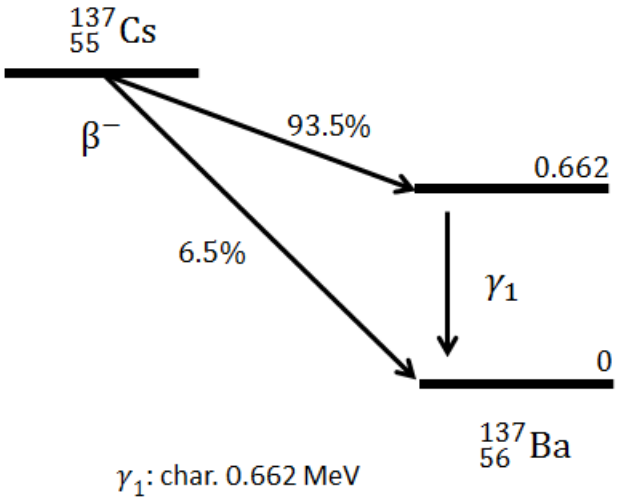

Figure 2-5 Beta-minus decay of ^{137}Cs [18]

Figure 2-5 shows an example of beta-minus decay of ^{137}Cs and its dominant excited energy state [18]. Following the beta-minus decay ^{137}Ba is in an excited state 93.5% of the time and emits a 662 keV gamma ray to relax to its ground state. The gamma ray emitted is called characteristic gamma radiation because observing the gamma radiation of this energy can be used to identify the radionuclide, while the intensity of the characteristic gamma ray can be used to identify the abundance of the radionuclide.

Figure 2-6 shows an example of the ^{137}Cs gamma spectrum measured from high purity germanium, a semiconductor radiation detector used for high-resolution gamma spectroscopy. The 662 keV peak represents the full energy photopeak. There is a Compton continuum starting at approximately 500 keV. Finally, the detector used in the figure was designed to identify 90º Compton scattering as evident by the peak at 373 keV.

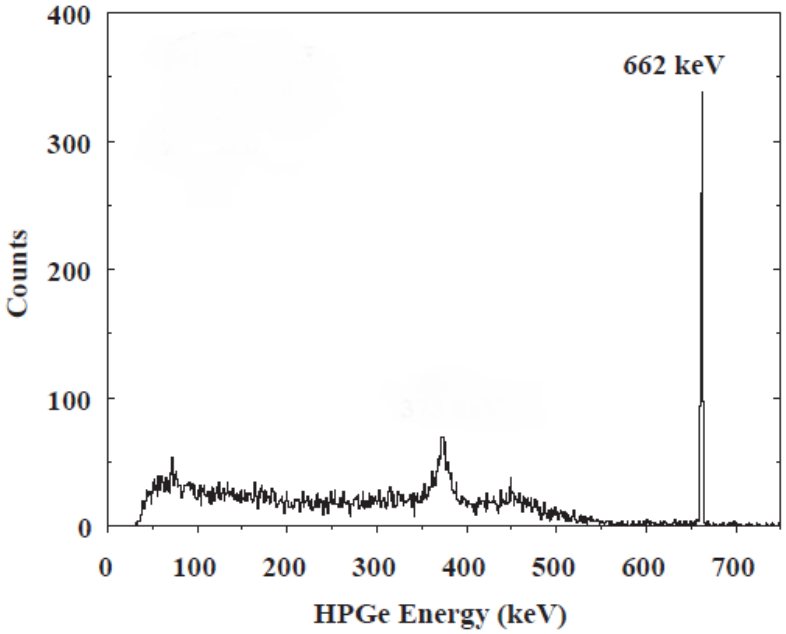

Figure 2-6 HPGe measurement of ^{137}Cs [19]

Measuring characteristic gamma radiation and relating that measurement to the underlying radionuclides which produced the radiation is the basis of gamma spectroscopy.

2.1.4 Radioactive Decay in DELFIC

Often the original fission products go through multiple decays before reaching a stable state. These are called decay chains. Tracking multiple decay chains and abundance of radionuclides present at a given time is modeled in DELFIC and ORIGEN-S through the Bateman equation [11]:

$$N_n(t) = \sum_{i=1}^{n} \sum_{k=1}^{n} c_{ki} * N_i^o * e^{-\lambda_k t} \quad \textbf{(2.2)}$$

where:

- $N_n(t)$ is the number radionuclides of the *n*th member of the chain at time t
- N_i^o is the number of radionuclides of the *i*th number of the chain ($i \leq n$) at time 0
- λ_k is the decay constant of the *k*th member of the chain ($k \leq n$)

The variable c_{ki} is defined as:

$$c_{ki} = \prod_{j=i}^{n-1} \lambda_j \Big/ \prod_{\substack{j=i \\ j \neq k}}^{n} (\lambda_j - \lambda_k) \quad \textbf{(2.3)}$$

This equation is applied to every radioactive daughter product produced by the initial detonation event to account for the composition of the fallout at later times. Given a concentration of any nuclide the activity is:

$$A_n(t) = \lambda_n N_n(t) \quad \textbf{(2.4)}$$

where:

- $A_n(t)$ is the activity of the nth radionuclide at time t (decays/sec)
- λ_n is the decay constant of the *n*th radionuclide

DELFIC uses the Bateman equation to produce a library of radionuclide inventories at various times. The radionuclide inventory is used in conjunction with ORIGEN-S's decay library to compute the gamma emission spectrum at various times.

2.2 Fractionation

The majority of the material in nuclear fallout is glassified soil and material surrounding the blast location. Fractionation is the term used to explain how fission products are distributed in this mostly inert material. Fractionation is defined as any alteration of radionuclide composition occurring between the time of detonation and the time of radiochemical analysis which causes the debris sample to be non-representative of the detonation products taken as a whole [5]. There are two types of fractionation: physical fractionation and chemical fractionation. One of the major contributors to gamma intensity variance is fractionation. If fractionation did not occur then the distribution of radionuclides in any sample measurement of fallout particles should follow the fission mass yield curve adjusted for any decay between the detonation and time of measurement. The definition is intentionally broad and applies to multiple physical phenomena that occur during and after a nuclear detonation ranging from the ambient air conditions to the chemical freezing temperatures of the fission daughter products.

2.2.1 Chemical Fractionation

Chemical fractionation refers to the alteration of the radionuclide composition in fallout due to vaporizing and subsequent freezing of the radionuclides and material from the surrounding environment. When a nuclear device detonates over land a substantial quantity of surrounding soil is lofted and vaporized. When the soil and all the surrounding material reach their freezing temperature, they condense to form fallout particles. Since the radionuclides of interest are radioactive and decaying into different elements, chemical fractionation behavior is often described in terms of isobars or "mass chains." Mass chain refers to a parent-daughter decay chain in which the mass number remains the same i.e. beta-minus decay. Chemical fractionation refers to how a radioactive mass chain is distributed in the fallout material itself. If the mass chain's freezing temperature is higher than the surrounding soils freezing temperature, the mass chain will be in the liquid or solid phase when the soil freezes. As a result these mass

chains tend to be *volumetrically* distributed in the fallout particle itself and are said to be "refractory." Mass chains which have a lower freezing temperature than the surrounding soil are still in the gaseous phase when the soil freezes and they condense on the *surface* of the fallout particles and are said to be "volatile." For some mass chains there is a mix of refractory and volatile elements in the mass chain. Differing detonation conditions cause a change in refractory/volatile ratio of a mass chain's distribution to change. This change is called the Freiling Ratio and is defined as the fraction of atoms that exist in the form of refractory elements at the time of soil solidification [20]. The Freiling Ratio is a way of quantifying the degree to which a mass chain undergoes chemical fractionation.

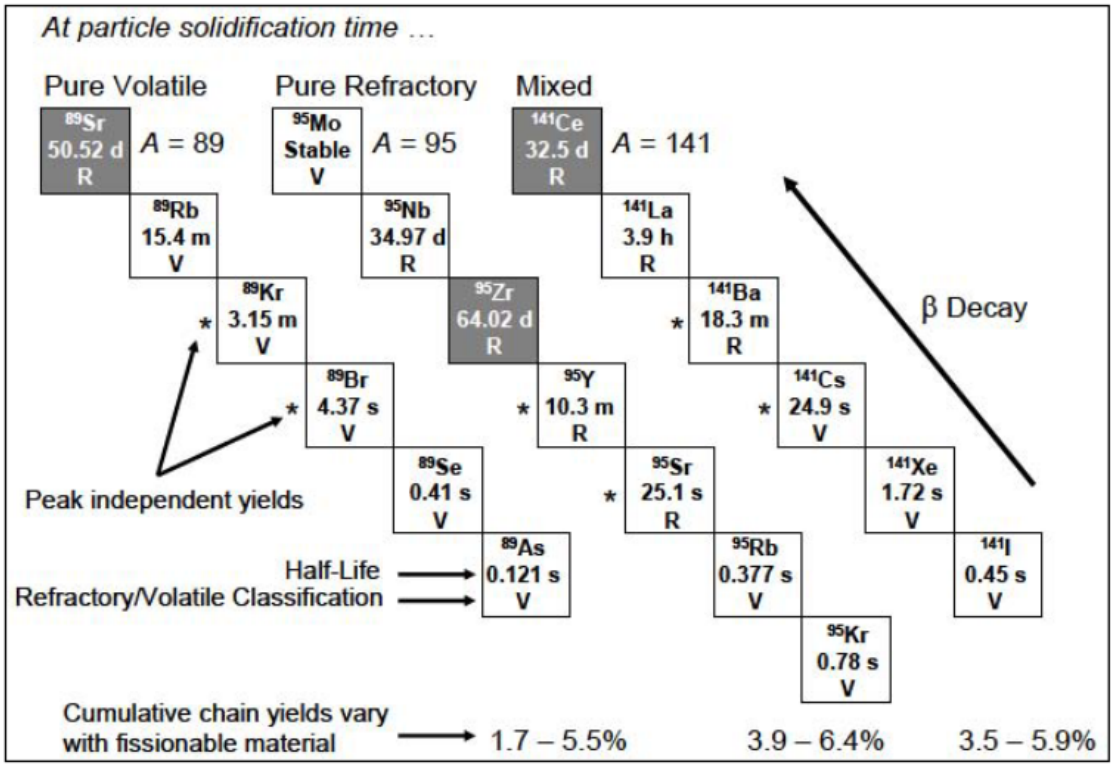

Figure 2-7 Mass chains exhibiting different degrees of chemical fractionation [21]

Figure 2-7 illustrates behavior of mass chains 89, 95, 141, and the behavior of each, for a specific soil solidification time [21]. One important note is that the mass chain behaviors illustrated are for a specific soil solidification time and can change as soil solidification time is changed.

Soil solidification time is important because it largely determines the degree of fractionation that the fallout particles exhibit. Solidification time can change according to several conditions. Izrael, et al. used the results exhibited in multiple Russian detonations to explain the factors that determine soil solidification time. His conclusion was that the nature of the environment where the device was detonated and the parameters of the device (the total explosive yield and the whether the device is detonated over water or land) primarily determine the radionuclide composition of fallout. Prevailing meteorological conditions only effect the quantitative distribution of fallout on the ground [17]. One of the device parameters that determine soil solidification time is total explosive yield. Total explosive yield determines how large and hot the fireball gets during the detonation. Higher explosive yields result in longer solidification times. The same behavior is exhibited, although with a weaker dependence, with burst height. As a device is detonated at altitude, less and less soil comes in contact with the fireball. Therefore, increasing detonation altitude from the surface decreases soil solidification time. There are other factors that contribute to solidification time like the composition of the soil and the ambient temperature at the time of burst. However for modeling purposes, environmental factors were treated as control parameters.

2.2.2 Physical Fractionation

Chemical fractionation pertains to how the radionuclide distribution changes as a function of the processes involved in vaporizing and freezing of fallout material. Physical fractionation refers to how the radionuclide composition deviates from the mass yield distribution due to the physical characteristics of the fallout. Larger diameter particles have a larger volume to surface area ratio than smaller particles. As a result, larger particles have a greater concentration of

refractory radionuclides than smaller particles. Another form of physical fractionation is the dispersion of fallout on the ground due to meteorological conditions (i.e. wind direction and speed.) Larger particles are more massive than smaller particles. As a result larger particles fall more quickly to the ground and closer to ground zero than smaller particles. This means higher concentrations of refractory radionuclides are closer to ground zero than volatile radionuclides.

2.2.3 Fractionation and Particle Modeling in DELFIC

DELFIC models the creation of particles and the degree of chemical fractionation in the initialization and cloud rise module (ICRM). The physical fractionation and the transport of particles to the ground is modeled in the Diffusive Transport Model (DTM). There are two principal assumptions used by DELFIC when modeling fallout particles. The first assumption is that fallout particles are spherical and homogenous with a lognormal distribution in size. Lognormally distributed particles are ones in which the logarithm of particle size is distributed normally. This is the default distribution used by DELFIC to determine particle size; however, there is an option to provide a custom distribution if desired. The second assumption is that the ultimate distribution of each mass chain among the particles is proportional to a power of the particle diameter [22].

The distribution of size of particles from a given simulation is given by:

$$D(x) = \frac{1}{\sqrt{2\pi} * \mathrm{x} * \ln s} \exp\left[-\frac{1}{2}\left(\frac{\ln x - \ln x_{50}}{\ln s}\right)^2\right] \tag{2.5}$$

Where:

- x is particle diameter
- s is geometric standard deviation of particle diameter (dimensionless)
- x_{50} is median diameter of particles
- $D(x)$ is the distribution of particles in diameter range dx

Equation (2.5) gives the distribution of particle sizes. In DELFIC the equation is generalized for arbitrary particle size distributions.

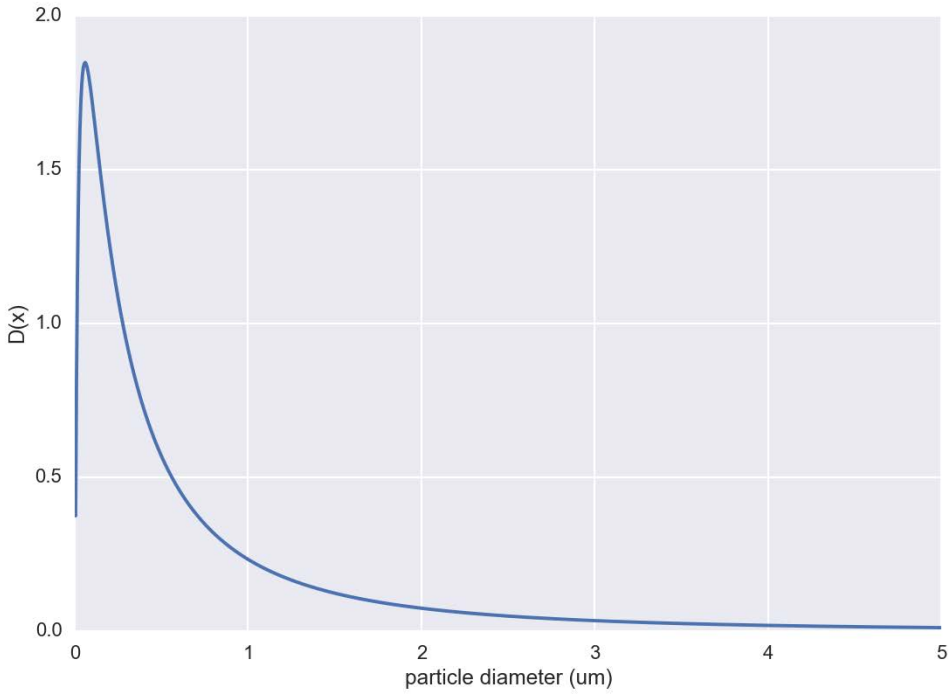

Figure 2-8 Lognormal distribution of particle diameter with mean $x_{50} = 0.407$μm and $s = 4.0$(dimensionless)

The next part of the simulation is to determine the degree of chemical fractionation (Freiling ratio) of the radionuclides. This is done by determining the time when the soil condenses and ceases to absorb radioactive radionuclides. Fission products that condense prior to soil solidification are distributed volumetrically through the particle. Fission products that condense after soil solidification are distributed over the surface. The formula used is semi empirical and takes into account the freezing point of the soil, total explosive yield, type of

material used, and the height of burst [11]. The radionuclide composition of fallout particles can vary widely based on any change in one of the aforementioned parameters. The sensitivity of Freiling ratio to different user inputs was examined by Miller in his dissertation [9]. He examined multiple soil freezing temperature, fissile materials, and soil solidification times. In all cases the changes in Freiling ratios were significant for multiple mass chains. This concludes a basic overview of how fallout particle size and the degree of fractionation are modeled in the initialization and cloud rise module of DELFIC. The last aspect of the simulation is how particles are transported from the cloud to the ground in DELFIC.

2.2.4 Diffusive Transport in DELFIC

How fallout particles are transported in DELFIC is important because it determines the physical fractionation of fallout samples. DELFIC first calculates the initial cloud rise, volume, temperatures, pressures, and density of fallout material. This is done for every particle size, so in effect, there are multiple "clouds." When each cloud reaches its stabilization point it is assumed to have uniform composition and be cylindrical in shape. It is then subdivided into "disks." See Figure 2-9 for an illustration. The direction and velocity of each disk is determined according to particle size, and position in the cloud. The meteorological data is then used to adjust the horizontal positions of the disks relative to ground zero. The disks are then transported to the ground in the diffusive transport module (DTM) of DELFIC. The DTM begins its calculation with the following information about the disks:

- Horizontal space coordinates of the parcel center
- Base altitude
- Stabilization time
- Vertical thickness
- Radius
- Mass

- Particle diameter
- Volume [11].

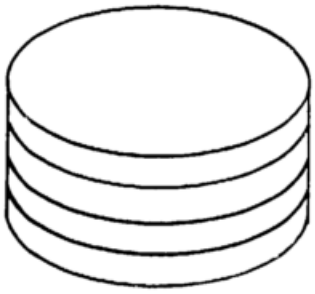

Figure 1. Subdivision of an initial cloud cylinder into four parcels, KDI = 4.

Figure 2-9 Example of cloud stem subdivision in ICRM prior to atmospheric transport [11]

The DTM combines this information with environmental conditions (atmospheric pressure, temperature, humidity, density, and viscosity) to transport the disk to their (x,y) position on the ground [11]. DELFIC allows user inputs for environmental conditions, or if a simulation for a previous date and time is desired, NOAA environmental data can be imported. Figure 2-10 shows a comparison of a measured fallout field with a fallout field recreated by DELFIC. DELFIC produced these results without a posteriori adjustment or calibration [11].

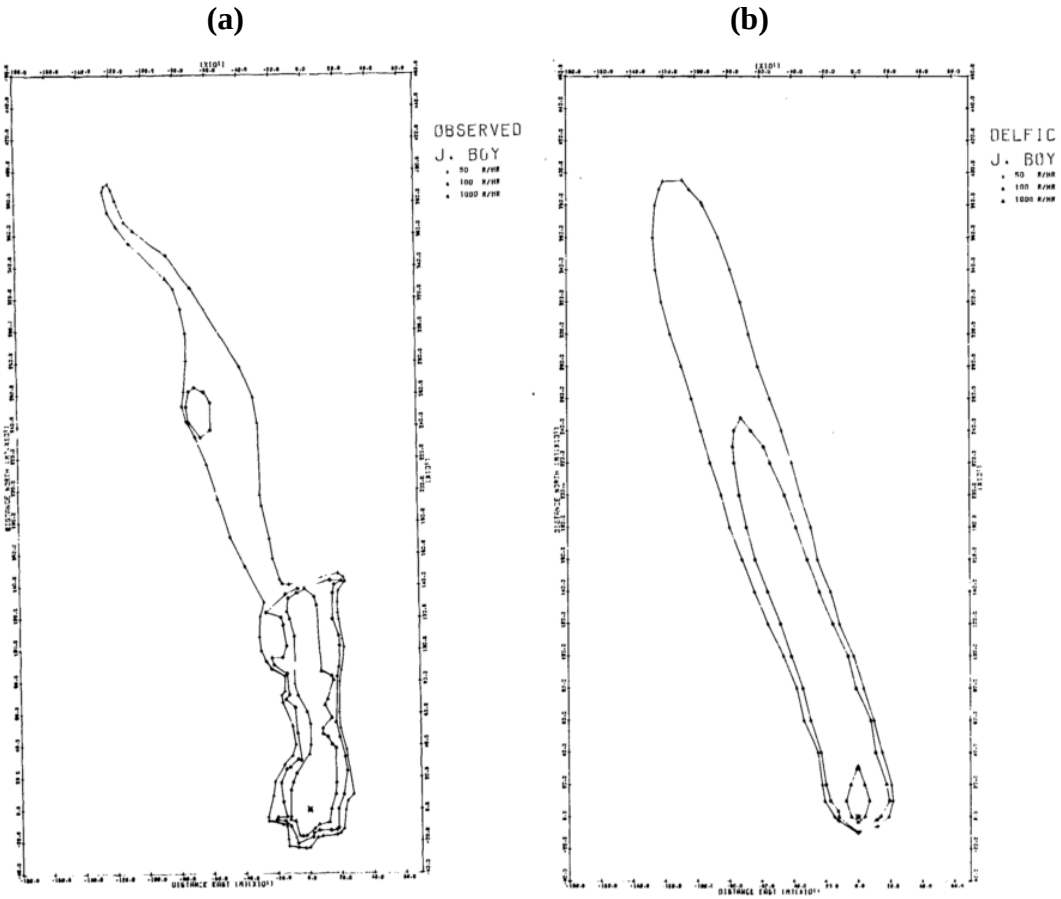

Figure 2-10 Comparison of DELFIC fallout field to observed nuclear detonation (a) observed fallout field of J. Boy nuclear test (b) DELFIC recreated J. Boy test [11]

This concludes the section on theory and modeling techniques. It covered the basic physical concepts of how radioactive material is produced during nuclear explosions and how fallout particles are created. Fractionation was also covered, which describes how radionuclides present in the fallout can change based on the chemical and physical properties of the fallout material. The last topic covered was DELFIC and a general overview of how simulation data is generated for the results section of the thesis.

2.3 Simulation Methods and Statistical Analysis

Our objective was to identify how to best distinguish nuclear detonation device characteristics using gamma spectroscopic measurements of fallout. The primary device characteristics of interest were the fissile fuel material and the energy of the neutrons used to induce fission. Specifically, we want to determine if gamma spectroscopy can be used to discriminate between differing combinations of nuclear fuel and neutron energy. The fuel options explored were ^{239}Pu, ^{235}U, and ^{238}U, and the two neutron energies analyzed were fast fission spectrum neutrons and high-energy neutrons (fusion neutrons).

2.3.1 Modeling Method in DELFIC

The first step was to randomly vary a single DELFIC input parameter while holding all other parameters constant. The input parameters that can be varied in DELFIC are listed in Table 2-1.

Table 2-1 DELFIC input parameters

Input Parameters
Total explosive yield (total yield): kilotons TNT (kt)
Fuel type: ^{239}Pu, ^{235}U, ^{238}U
Neutron energy: Fission spectrum or fusion spectrum
Height of Burst: meters (m)
Wind: Speed (meters/second), direction (degrees, with 0º being North)

Soil type is also an input parameter; however for the scope of this research only land detonations were examined. This was modeled in DELFIC as the default “siliceous soil” option.

DELFIC then took the input parameters and generated a radionuclide inventory of fission daughter products and activated soil products. The corresponding gamma spectrum was calculated using the ORIGEN-S gamma yield database. The results of the simulation can be viewed under the conditions listed in Table 2-2.

Table 2-2 Simulation observation conditions of gamma ray intensity

Gamma ray energy (keV) /characteristic nuclide(e.g. ^{112}Ag)
Sample location relative to ground zero in kilometers (km)
Fallout particle size diameter in micrometers(μm)
Fallout collection time (hours since detonation)

This gave the user a unique set of gamma spectra for every instance of the varied input parameter. The set of gamma spectra was then modeled using linear regression. Sensitivity to the input parameters was evaluated using the F-Test.

Two notable input parameters are fissile fuel material and the neutron flux energy. The combination of these two parameters result in a categorical variable referred to as "Fission Type." Table 2-3 lists the definition of the six categorical variables that are selectable in DELFIC.

Table 2-3 Table of variables for "Fission Type" input parameter

	fuel material		
	^{235}U	**^{238}U**	**^{239}Pu**
fission spectrum neutrons	u235fi	u238fi	p239fi

fusion spectrum neutrons	u235he	u238he	p239he

The focus of the research was to isolate the gamma lines (and their associated characteristic nuclides) that gave the most information about fission type. Gamma ray intensities are derived directly from the radionuclides that are emitting them.

The first two observables examined were particle size and sample location. This was done to examine the effects of physical fractionation as discussed in section 2.2.2. The next step was to perform linear regression for every gamma line present in the spectrum. This was accomplished in three experimental simulations. The first simulation varied total explosive yield while fixing the burst height. The next simulation varied burst height while fixing total explosive yield. The last simulation varied both burst height and total explosive yield. Useful gamma lines were then identified by ranking the gamma lines by the maximum standard deviation and maximum/minimum separation between the normalized gamma intensity as predicted by the regression model. Finally, the same analysis was performed on a variety of fallout collection times to provide a general overview of the best gamma lines for distinguishing fission type.

2.3.2 Statistical Modeling of Parameters

Statistical modeling used normalized (the intensity of each gamma line was normalized to the total intensity of all gamma lines in the spectrum) gamma spectra as a response to multiple input variables. One finding of this thesis is that controlling particle size of fallout particles reduces the variance of the normalized gamma spectra to such a degree that linear regression is a suitable approach to modeling the simulation results. Figure 2-11 illustrates the effect controlling particle size has on normalized gamma intensity. In this case the independent variable was total

explosive yield. Both figures are from the 743.4 keV gamma decay of ^{97}Zr, the details of which will be discussed further in the results section. It is important to note that Figure 2-11(a) is the intensity for all particle sizes, while Figure 2-11(b) is the intensity for only 490-510 µm particles. Note that controlling particle size virtually eliminates variance in composition. The remaining variance is primarily due to fission type. Figure 2-11 (b) exhibits linear behavior hence linear regression analysis was used to analyze the data. At first glance it appears that the intercept can be used to categorize fission type since the slopes of the lines are small compared to the separation between the fission types.

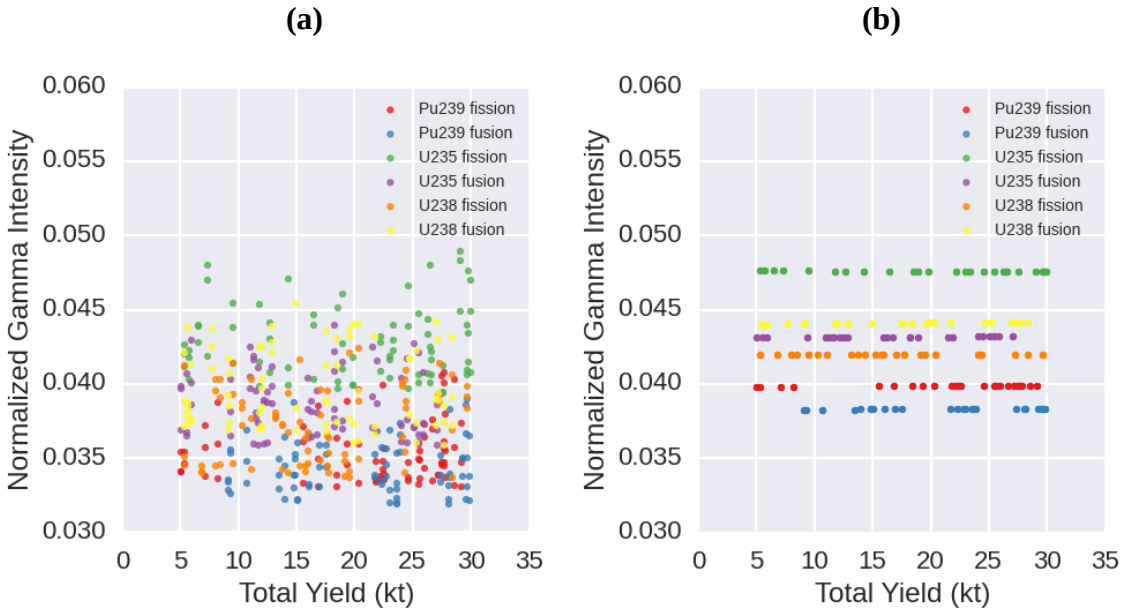

Figure 2-11 Normalized 743.4 keV gamma intensity for (a) all particle sizes in fallout (b) 490-510 µm particles

The response variable for our analysis is normalized gamma intensity while the regressor variables are the DELFIC input variables: total explosive yield, height of burst, and fission type. The only DELFIC input variable not modeled using linear regression was wind speed and direction. This was analyzed as sample location in the fallout field, since wind speed and direction directly affect the location of where fallout particles land. Since fission type was the primary regressor variable of interest, it was modeled during the *varying total explosive yield* simulation and *varying burst height* simulation. All models included interaction coefficients between the regressor variables being analyzed. Equation (2.6) shows the form of the regression model used to analyze all DELFIC simulations.

$$Y_i = \beta_{00} + \sum_{j=1}^{6} (\beta_{0j} + \beta_{1j} * x_i) z_{ij} + \epsilon_i \qquad (2.6)$$

where:

- i is the simulation number
- j is fission type
- x_i is yield or burst height of i th observation
- Y_i is normalized gamma intensity
- z_{ij} is a delta function with values: $\begin{cases} 1 & \text{if test } i \text{ is fissiontype } j \\ 0 & \text{otherwise} \end{cases}$
- β_{00} is the intercept model coefficient
- β_{0j} is the fission type model coefficients
- β_{1j} is either total explosive yield or burst height model coefficients
- ϵ_i is random error in the model

Total explosive yield and burst height are treated as continuous random variables. Fission type is treated as a categorical variable with 6 possibilities called “levels.” Categorical

independent variables are modeled in regression using binary 1 or 0 in the design matrix used to estimate the mode. This is represented by z_{ij}, where z_{ij} is 1 when the DELFIC simulation i is fission type j and 0 otherwise.

2.3.3 The F-Test

Once the regression models were constructed, a test for the significance of regressor variables was performed using the F-Test. The F-test for regression models is a statistical test used to make statements about significance of regression model parameters. To perform the test some model coefficients were assumed to be 0 and the data was fit to this model (referred to as the "reduced" model.) Then the variance introduced by changing the model is compared to the original "full" model. This is expressed as the null hypothesis.

- Null Hypothesis: $\beta_1 = 0$ for every level j
- Alternate Hypothesis: $\beta_1 \neq 0$ for some j

Applying the hypothesis to equation (2.6) yields the following equation:

$$Y_i = \beta_{00} + \sum_{j=1}^{6} \beta_{0j} * z_{ij} + \epsilon_i \tag{2.7}$$

where:

- i is the simulation number
- j is fission type
- x_i is yield or burst height of i th observation
- Y_i is normalized gamma intensity
- z_{ij} is a delta function with values: $\begin{cases} 1 & \text{if test } i \text{ is fissiontype } j \\ 0 & \text{otherwise} \end{cases}$
- β_{00} is the intercept model coefficient
- β_{0j} is the fission type model coefficients
- β_{1j} is either total explosive yield or burst height model coefficients

- ϵ_i is random error in the model

Equation (2.7) applies the null hypothesis that the slope versus total explosive yield or burst height is zero. For all the simulations tested, Equation (2.7) is the reduced model whereas the Equation (2.6) is full model.

A different hypothesis was tested for the final simulation. This was one where total explosive yield and/or burst height is known. In an actual nuclear detonation this would represent a case where yield and burst height is calculated by means other than gamma spectroscopy (size of crater, height of mushroom cloud, etc.). The test in this case was whether the model coefficients for fission type are the same given knowledge of burst height and total explosive yield. To model this special case let:

$$w_i = x_i - x_o \tag{2.8}$$

Where:

- x_o is the known yield or burst height
- w_i is the difference between the x_i observation and the known yield or burst height

The reduced model is then defined as:

$$Y_i = \beta_{00'} + \sum_{j=1}^{6} (\beta_{0j'} + \beta_{1j'} * w_i) z_{ij} + \epsilon_i \tag{2.9}$$

Where:

- i is the simulation number
- j is fission type
- w_i is the difference between the x_i observation and the known yield or burst height
- Y_i is normalized gamma intensity

- z_{ij} is a delta function with values: $\begin{cases} 1 & \text{if test } i \text{ is fissiontype } j \\ 0 & \text{otherwise} \end{cases}$
- β_{00}, is the intercept model coefficient given w_i
- β_{0j}, is the fission type model coefficients given w_i
- β_{1j} is either total explosive yield or burst height model coefficients
- ϵ_i is random error in the model

Here we have β_{00}, and β_{0j}, as the new model coefficients. The hypotheses tested in this case then become:

- Null Hypothesis: $\beta_{0j} = \beta_{0j}$, for all j, j'
- Alternate Hypothesis: $\beta_{0j} \neq \beta_{0j}$, for some j, j'

The F-Test is then used to compare the reduced models to the full model. The F-Statistic is as follows:

$$F = \frac{SSR/_{DFR}}{SSE/_{DFE}} \tag{2.10}$$

Where:

- SSR is the sum of squares for the regression
- SSE is the of squares for the residuals
- DFR is degrees of freedom for the regression
- DFR is degrees of freedom for the residuals

The F-value is a comparison of the explained variance and the unexplained variance. Equation (2.11) represents the F-value for a regression model:

$$F = \frac{\left(\frac{SSR_{red} - SSR_{full}}{DF_{red} - DF_{full}}\right)}{\left(\frac{SSR_{full}}{DF_{full}}\right)} \tag{2.11}$$

Where:

- SSR_{red} is sum of squares for the reduced model
- $SSR_{full}$is sum of squares for the full model
- DF_{red} is degrees of freedom for the reduced model (# of observations - # of parameters)
- DF_{Full} is degrees of freedom for the full model (# of observations - # of parameters)

Again we are measuring the ratio between the explained and unexplained variance. This is done by calculating the difference in sum of squares between the reduced model and the full model scaled by the change in model coefficients. This F-Value can then test for significance level α using the F(x, DF Numerator, DF Denominator) distribution.

$$F(x; d_1, d_2) = \frac{\sqrt{\frac{(d_1 * x)^{d_1} * d_2^{d_2}}{(d_1 * x + d_2)^{d_1+d_2}}}}{x * B\left(\frac{d_1}{2} + \frac{d_2}{2}\right)}$$

Where:

- d_1 is the degrees of freedom in numerator of the F-Value
- d_2 is the degrees of freedom in the denominator of the F-Value
- B is the beta function

Figure 2-12 is a plot of the F-distribution probability density function with the degrees of freedom used in the simulation.

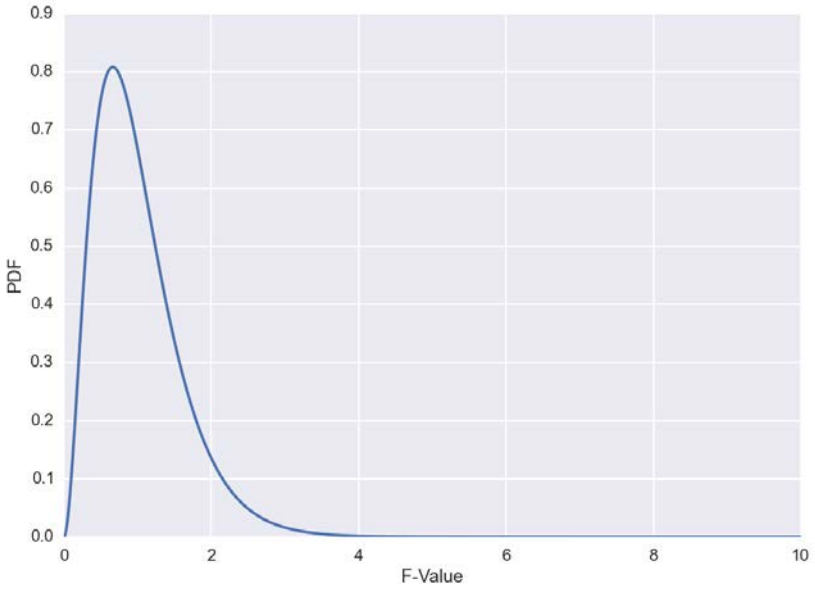

Figure 2-12 F-distribution used for ANOVA

This allows us to compute the probability that the F-value of the distribution will be larger than the observed F-value. Following the F-Test, the final analysis done was to rank how well each gamma line discriminates between each fission type.

Useful gamma lines were ranked by the maximum standard deviation and maximum/minimum separation between the normalized gamma intensity as predicted by the regression model. For the test cases the intercept value of the regression model was used for comparison since there was such a weak dependence on total explosive yield. However if the total explosive yield was known or could be approximated by other means that value could be used in the model to rank normalized gamma intensities.

3 Results and Discussion

DELFIC simulations were performed to systematically vary the fission type categorical parameter while randomly varying the other continuous parameters, i.e. explosive yield, burst height, and fallout collection location. The intent was to identify gamma spectrum photopeaks that could be used to categorize fission type and were simultaneously insensitive to other randomly varying parameters. Similar analyses have been performed in the past; however the current results perform the analysis while controlling fallout particle diameter (particle size). All input parameters for DELFIC are:

- Fission type
- Total explosive yield
- Burst height[1]

The properties affecting gamma ray intensity in collected fallout particles are:

- Gamma line energy
- Sample location
- Fallout particle diameter
- Fallout collection time

3.1 Conditions Affecting the Gamma Spectrum

The following examples serve to illustrate in a broad sense how the gamma spectrum changes as a function of different input parameters in DELFIC. Listed on the x-axis in each

[1] Soil type, wind direction, and wind velocity are also input parameters but were not varied in the simulation. Soil type was assumed to be siliceous for domestic detonations. Wind speed and velocity only effects sample location of fallout and was accounted for by varying sample location.

subsequent plot is the energy of the gamma rays being released by various radionuclides in the fallout particles, these are referred to as gamma lines. Listed on the y-axis is the intensity of each gamma line, measured in gamma rays released per second. As discussed in section 2.1.4 the gamma spectrum is a direct observation of the abundance and decay properties of the radionuclide composition of the fallout.

3.1.1 Gamma Spectra from Varying Neutron Energy

Figure 3-1 shows the gamma spectra of a nuclear device in which fission is induced by neutrons from two different neutron energy distributions. Recall, fission induced by high energy neutrons produces daughter products with a more shallow "saddle" in the fission mass yield curve. In this example the fuel is ^{239}Pu. Figure 3-1 (a) shows the gamma spectra resulting from fission events induced by neutrons in the prompt fission neutron energy spectrum. Figure 3-1 (b) shows the gamma spectrum resulting from fission events induced by neutrons from nuclear fusion. The presence of certain gamma lines as well as their ratio to other gamma lines is referred to as the shape of the spectrum. This shows how gamma spectra differ between devices detonated using different neutron energies.

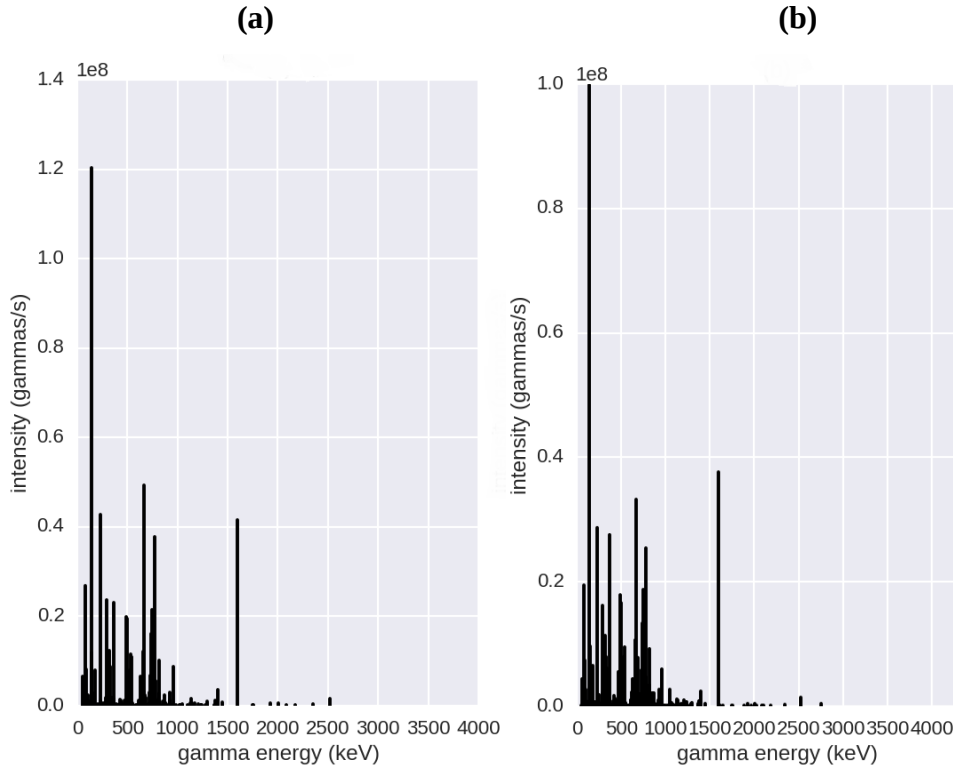

Figure 3-1 Gamma spectrum from detonation events of differing neutron energies (a) spectra from fission neutrons energies (b) spectra resulting from fusion neutron energies

3.1.2 Gamma Spectra from Varying Fuel Material

Figure 3-2(a) is the spectrum from a device made with ^{239}Pu, while (b) is from a device made with ^{235}U. Recall, ^{239}Pu has a higher mass number than ^{235}U so the fission product mass yield curve is "shifted" to the right for ^{239}Pu. Similar to spectra from different neutron energies, the spectrum is different between different types of fuel. When comparing the spectrum shapes of Figures (a) and (b) we can see that some gamma lines are present while others are not present. Another difference is that gamma line magnitudes are different at certain energies. Lastly the ratio between gamma lines is different for some gamma energies. This shows how gamma spectra differ between devices detonated using different fissile material.

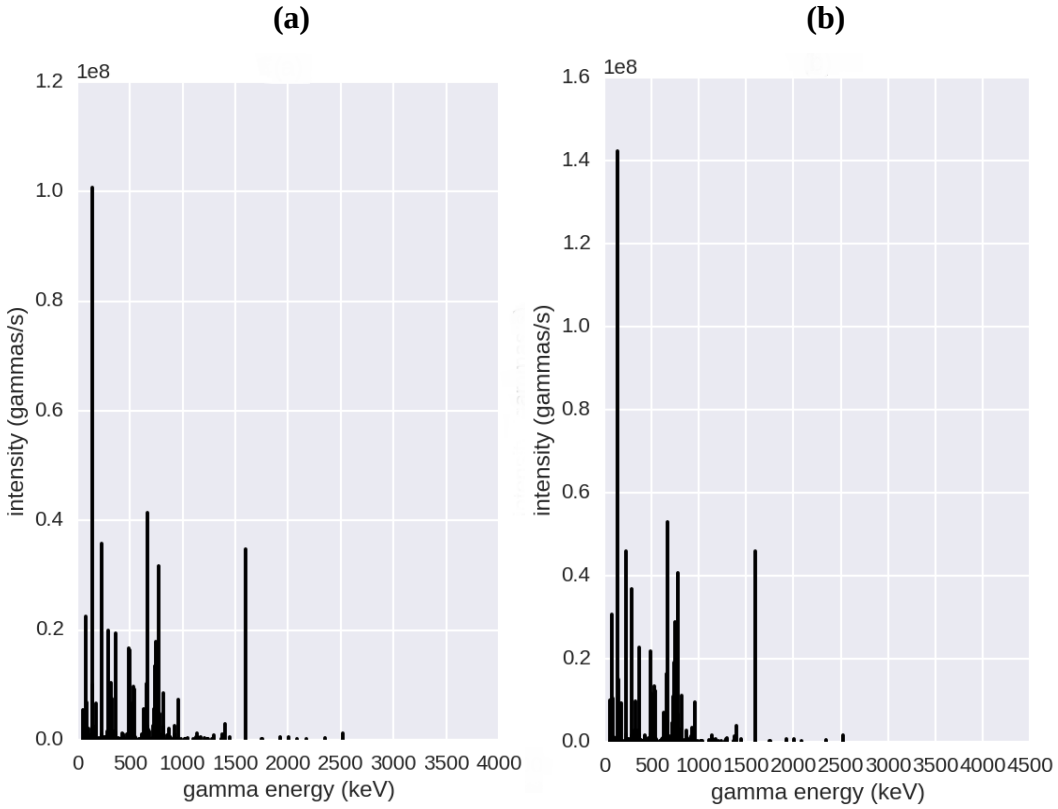

Figure 3-2 Gamma spectrum from detonation events of differing fuel types (a) device made with ^{239}Pu fuel (b) device made with ^{235}U fuel

3.1.3 Gamma Spectra from Varying Sample Location

Figure 3-3 shows gamma spectra from different sampling locations. Ground zero is defined as the location where the device is detonated. The difference in spectra is primarily because of atmospheric transport of fallout material.

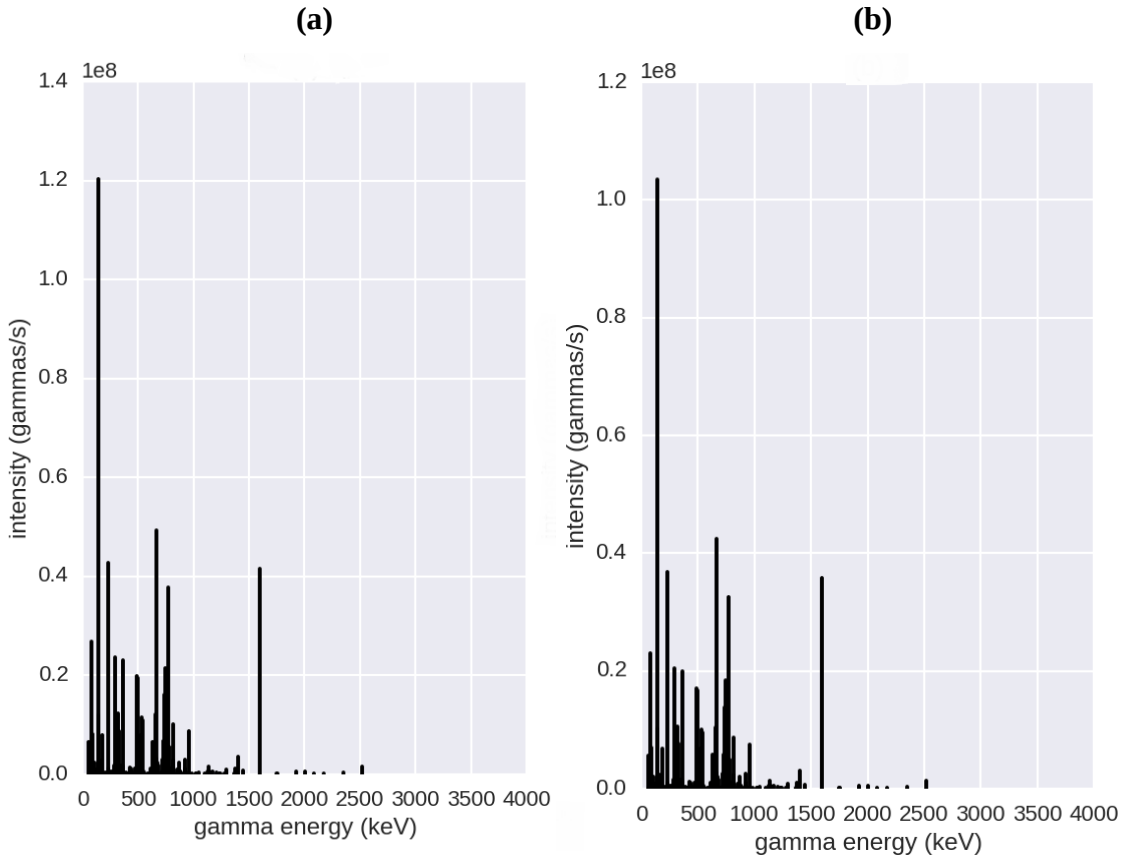

Figure 3-3 Gamma spectra from fallout collected at different locations (a) collection location 5.2 km from ground zero (b) collection location 7.3 km from ground zero

There are two reasons for the change in spectra between Figures (a) and (b). Larger heavier particles are concentrated closer to ground zero, while smaller lighter particles are lofted higher and carried further. Likewise, the total amount of fallout material available for collection is

generally found concentrated closer to ground-zero. As collection location moves away from ground zero, fallout generally becomes more dispersed.

Randomly varying sample location was accomplished by using DELFIC maps of exposure rate (DELFIC map type 3) and density of fallout particles (DELFIC map type 11 for all particles or 13 for select particle size). Only locations that had a dose less than 1.5 Roentgens/hour and a fallout density greater than 10 g/m^2 were sampled. This allows for a collection team to identify the areas that maximize the amount of fallout collected while minimizing radiation exposure.

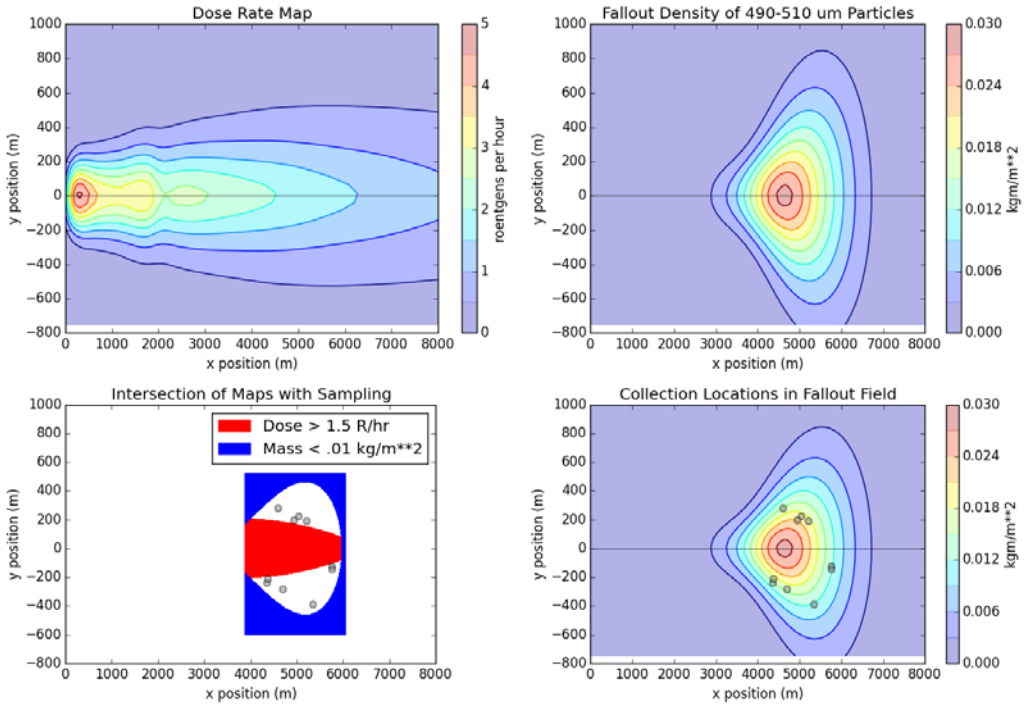

Figure 3-4 Fallout maps used to determine sample location using the intersection of dose rate and fallout density maps

3.1.4 Gamma Spectra from Varying Collection Time

Following a fallout event, gamma spectra change drastically as radionuclides with short half-lives decay away. Figure 3-5 is perhaps the most dramatic change in the gamma spectrum. At 2 days after detonation, radionuclides with half-lives close to the measurement time are some of the largest contributors to the spectrum. At 5 days after detonation, those same radionuclides have weak intensities since they have decayed away. Consequently, identifying the time the device is detonated is one of the most important pieces of information to have when attempting to accurately conduct gamma spectroscopy of nuclear fallout.

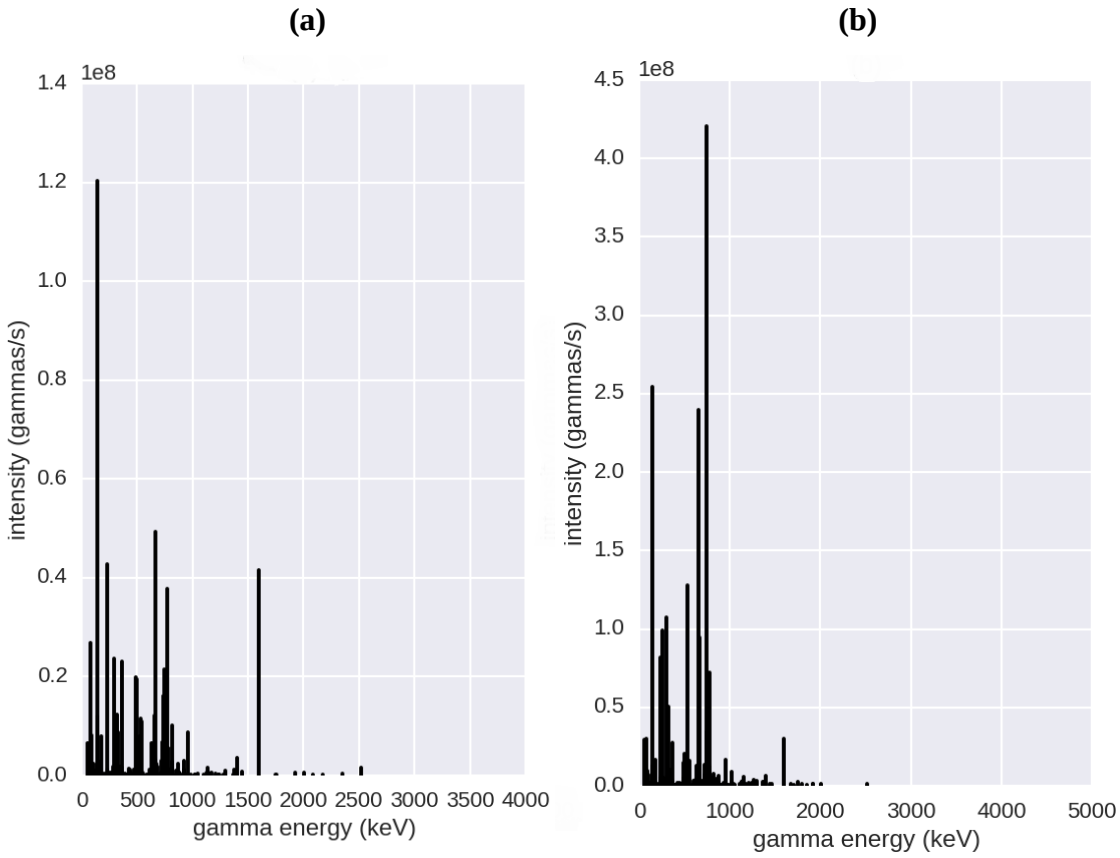

Figure 3-5 Gamma spectra from fallout collected at different times (a) collection time 5 days after detonation (b) collection time 2 days after detonation

Fission type, collection location, and collection time are just three examples of how gamma spectra changes and a function of different input parameters and observation conditions. This section presented those changes and introduced gamma spectra results output by DELFIC and ORIGEN for different detonation events. The next step in the simulation was to refine the spectra and identify the gamma lines that are useful for analysis.

3.2 Removing Low Energy and Low Intensity Gamma Lines from the Spectrum

Before analyzing every gamma line in the spectrum we removed lines which would be indistinguishable. Conservative removal criteria were used.

- Gamma energies less than 50 keV were removed
- Gamma intensities less than 10^{-6} of total intensity were removed
- Gamma lines that were overlapping by full width ten-thousandth max were removed

Figure 3-6 shows: (a) original source spectra and (b) the retained spectra after the indistinguishable gamma lines are removed. The red lines in figure (b) are those which were removed before conducting analysis. This treatment of the gamma spectrum is used for the remainder of the paper. Any gamma lines reported are those retained after using the above removal criteria.

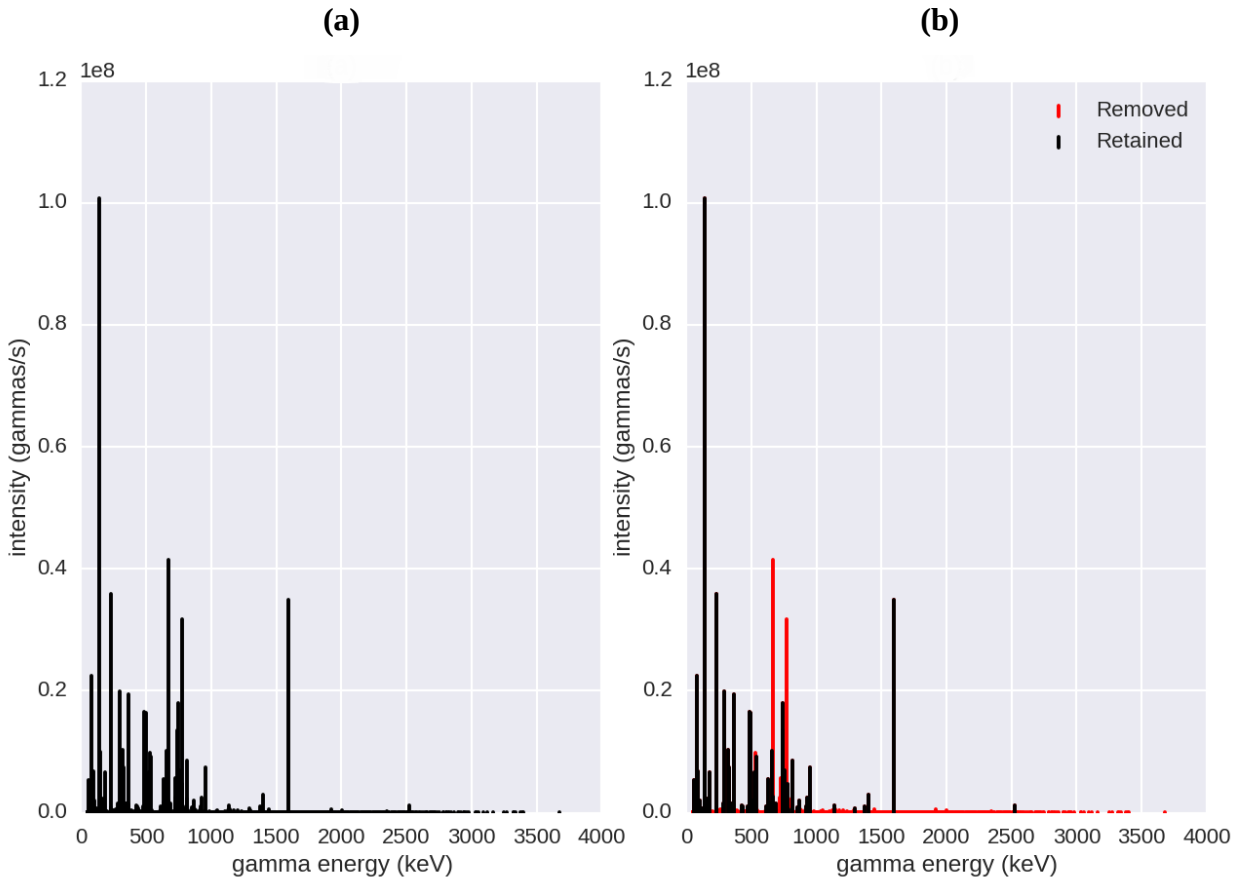

Figure 3-6 Gamma spectra removal of indistinguishable gamma lines (a) original spectrum (b) spectrum after indistinguishable lines were removed

3.3 Varying Sample Location

As mentioned before, isolating the fallout particle size is the basis for all spectra analyses in this thesis. Sample location is the first parameter varied in order to examine the effect controlling particle size has on gamma spectra. The expectation is that if identically sized particles are collected, the gamma spectra will be nearly identical. This is because controlling particle size removes radionuclide variance caused by physical fractionation. DELFIC inputs affecting sample location are wind direction, atmospheric pressure, and relative humidity.

Table 3-1 Model parameters for sample location simulation

Parameters	Model Scenarios
Fission Type	6 Types： (^{239}Pu, ^{235}U, ^{238}U) x (Fission and Fusion)
Yield (kt)	10
Sample location*	15 samples*
Burst Height (m)	1
Time after blast (d)	5
Particle size (μm)	490-510

* Parameter varied for simulation

For the first simulation 15 different locations and all 6 fission types were sampled. Each sample location consists of the total mass of 490-510 μm fallout particles that would fall in a one square meter area. All other parameters were held constant for the simulation. Table 3-2 and Table 3-3 show the radionuclides that have the highest gamma intensity for the simulation. Note this ranking applies only for the model scenarios listed in Table 3-1.

Table 3-2 Rank of top 15 gamma intensity sources for fission energy neutrons

Fission Neutron Energy Radionuclide, Peak Energy(keV), Normalized Gamma Intensity									
Rank	**^{239}Pu**			**^{235}U**			**^{238}U**		
1	Mo99	140.5	0.223	Mo99	140.5	0.232	Mo99	140.5	0.231
2	Te132	228.2	0.080	La140	1596.2	0.076	Te132	228.2	0.079
3	La140	1,596.2	0.077	Te132	228.2	0.075	I132	772.6	0.070
4	Xe133	81.0	0.050	Ce143	293.3	0.061	La140	1596.2	0.061
5	Ce143	293.3	0.044	Xe133	81.0	0.050	Xe133	81.0	0.048
6	I131	364.5	0.043	Zr97	743.4	0.048	Ce143	293.3	0.045
7	Zr97	743.4	0.040	I131	364.5	0.037	Zr97	743.4	0.042
8	La140	487.0	0.037	La140	487.0	0.036	Ru103	497.1	0.037
9	Ru103	497.1	0.036	Mo99	739.5	0.031	I131	364.5	0.036
10	Mo99	739.5	0.030	Nb97	657.9	0.027	Mo99	739.5	0.031
11	Rh105	318.9	0.023	Ce141	145.4	0.025	La140	487.0	0.029
12	Nb97	657.9	0.023	Zr95	756.7	0.022	Nb97	657.9	0.024
13	Ce141	145.4	0.022	Ba140	537.3	0.020	Nd147	91.1	0.020
14	Ba140	537.3	0.021	La140	815.8	0.019	Ce141	145.4	0.017
15	La140	815.8	0.019	Ru103	497.1	0.018	Zr95	756.7	0.017

Table 3-3 Rank of top 15 gamma intensity sources for fusion energy neutrons

Fusion Neutron Energy Radionuclide, Peak Energy(keV), Normalized Gamma Intensity									
Rank	**Pu239**			**U235**			**U238**		
1	Mo99	140.5	0.203	Mo99	140.5	0.213	Mo99	140.5	0.236
2	La140	1,596.2	0.077	La140	1596.2	0.076	Te132	228.2	0.079
3	Te132	228.2	0.058	Te132	228.2	0.070	La140	1596.2	0.059
4	I131	364.5	0.056	I131	364.5	0.051	I131	364.5	0.048
5	Xe133	81.0	0.040	Xe133	81.0	0.044	Xe133	81.0	0.048
6	Zr97	743.4	0.038	Zr97	743.4	0.043	Zr97	743.4	0.044
7	La140	487.0	0.037	Ce143	293.3	0.043	Ce143	293.3	0.042
8	Ru103	497.1	0.034	La140	487.0	0.036	Mo99	739.5	0.032
9	Ce143	293.3	0.033	Mo99	739.5	0.028	Ru103	497.1	0.030
10	Mo99	739.5	0.027	Nb97	657.9	0.025	La140	487.0	0.028
11	Rh105	318.9	0.023	Ce141	145.4	0.022	Nb97	657.9	0.025
12	Nb97	657.9	0.022	Ba140	537.3	0.020	Zr95	756.7	0.018
13	Ce141	145.4	0.020	Ru103	497.1	0.019	Nd147	91.1	0.017
14	Ba140	537.3	0.019	Zr95	756.7	0.019	Ce141	145.4	0.017
15	La140	815.8	0.019	La140	815.8	0.019	I132	954.6	0.016

The ^{99}Mo (in secular equilibrium Tc-99m) with gamma line 140.5 keV is the most active in all cases with approximately 20% of all the gamma emission being the 140.5 keV gamma line. Overall, the top 15 gamma lines in the spectra account for approximately two thirds of all gamma emissions. At each sample location in the simulation, gamma ray intensities were calculated and normalized. Normalization of the spectrum was accomplished by dividing the intensity of each gamma line by the total intensity of all gamma lines. The result was that each gamma line was expressed as a fraction with the total of all gamma line fractions summing to one. The normalization allows for a comparison of the gamma spectrum shapes at different sampling locations.

To compare the effect of controlling particle size, the relative uncertainty between the 15 unique gamma intensity measurements was calculated. Figure 3-7(a) shows the results when all

particle sizes contribute to the measurement. The relative uncertainties vary and are all non-zero. A relative uncertainty of 0.005 represents approximately 40,000 counts in a photopeak for the gamma intensities observed in the simulation. For many gamma lines, requiring 40,000 counts would require excessively long counting times. In Figure 3-7(b) we see that the relative uncertainty is near-zero when you only measure particles of a single size. This illustrates that if you control particle size, the gamma spectrum shape changes very little, regardless of the effects of atmospheric transport. The results presented are from ^{235}U fission neutron fission type. The same effect holds true for all other fission types.

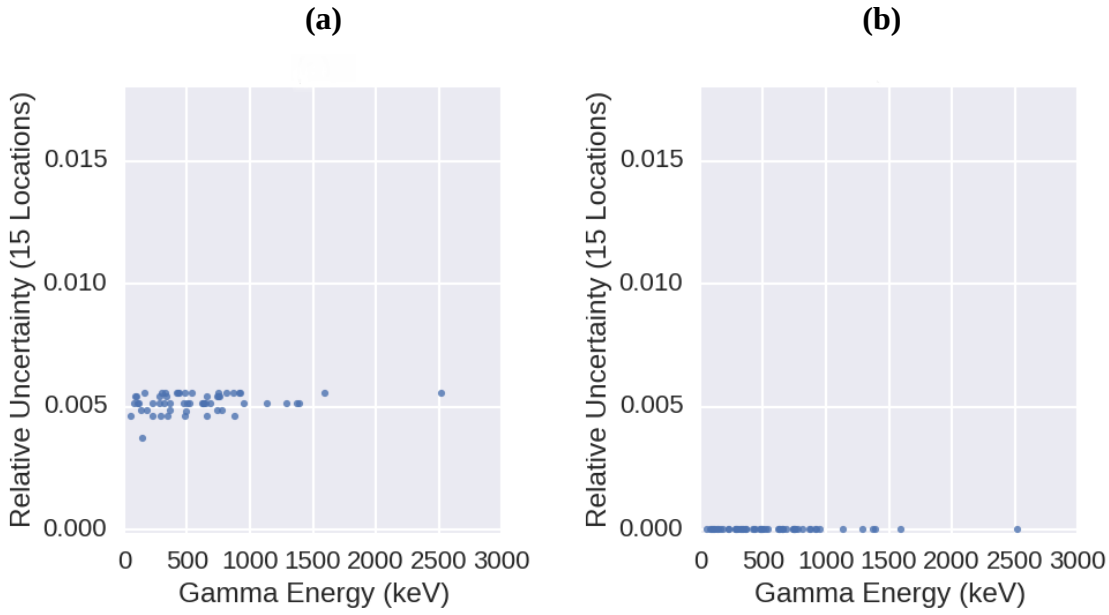

Figure 3-7 Relative uncertainty of gamma intensity between 15 sample locations (a) measurements of all particle sizes (b) measurements of fallout particles 490-510 µm in diameter

3.4 Varying Total Explosive Yield

The next effect examined was explosive yield. Explosive yield refers to total energy release from a nuclear detonation. Units for explosive yield are reported in tons TNT explosive equivalent, with most nuclear blasts in the kiloton to megaton range. For the remainder of the section the term "total yield" will refer to the total explosive yield of a nuclear detonation.

Table 3-4 Parameters used for testing gamma intensity as a function of total yield

Parameters	Simulation Inputs
Fission Type	6 Types : (^{239}Pu, ^{235}U, ^{238}U)x (Fission and Fusion)
Total Yield (kt)*	Range of 5-30, 25 samples*
Sample locations	3
Burst Height (m)	1
Time after blast (d)	5
Particle size (μm)	490-510

* Parameter being analyzed

For this simulation all other parameters were held constant, except for sample location. Table 3-4 shows the parameters being used for the simulation. 25 random total yield values were used and fallout was analyzed at 3 random sites. This was done for every fission type, producing 450 unique gamma spectra to analyze. Random sampling was drawn from a uniform distribution with a minimum of 5 kt and a maximum of 30 kt. To better visualize the effect of yield, each gamma line was examined individually.

Figure 3-8 is the 140.5 keV gamma line of Molybdenum-99 (^{99}Mo.) Figure 3-8 (a) shows the normalized gamma intensity of 140.5 keV when all particle sizes are analyzed. Figure 3-8 (b) shows the normalized gamma intensity of 140.5 keV when only 490-510 μm particles are

analyzed. Controlling particle size reduces the variance in normalized gamma intensity so much that each data point in Figure 3-8 (b) represents the normalized intensity at three sample locations and is indistinguishable from each other at this scale. Note the error bars are smaller than the data points themselves. ^{99}Mo was chosen because it is the most active gamma emitter, accounting for approximately 20% of the overall gamma emissions. It also happens to be one of the best gamma lines identified during this analysis to distinguish fission type. Another feature of the graph to note is the dependence of gamma intensity on total yield. For this gamma line, as yield increases, normalized gamma intensity decreases for this radionuclide. Since it is a normalized spectrum, the amount of ^{99}Mo decreases relative to all other radionuclides as yield increases. This dependence is most likely explained by chemical fractionation. As discussed in section 2.2.1, as yield increases soil solidification time also increases. This will affect the radionuclide composition of the fallout being analyzed.

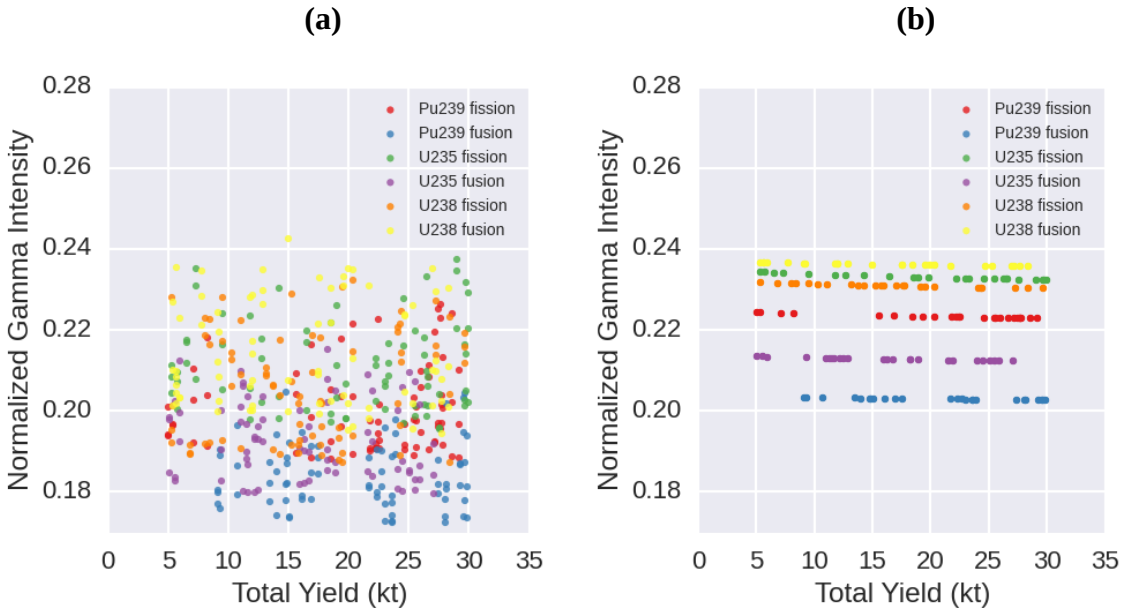

Figure 3-8 Normalized gamma intensity of 140.5 keV (^{99}Mo) as a function of fission type and total yield (a) all particle sizes in fallout (b) controlling particle size of fallout

To determine whether the dependence of normalized gamma intensity on total yield was statistically significant, the F-Test was used. The data was modeled using linear regression analysis. This was done for every gamma line. A simple interpretation of the linear regression parameters is that β_{0j} parameters are the estimated intercepts and, β_{1j} parameters are the estimated slopes. For illustrative purposes, the results for the ^{99}Mo 140.5 keV line are listed below:

(a)

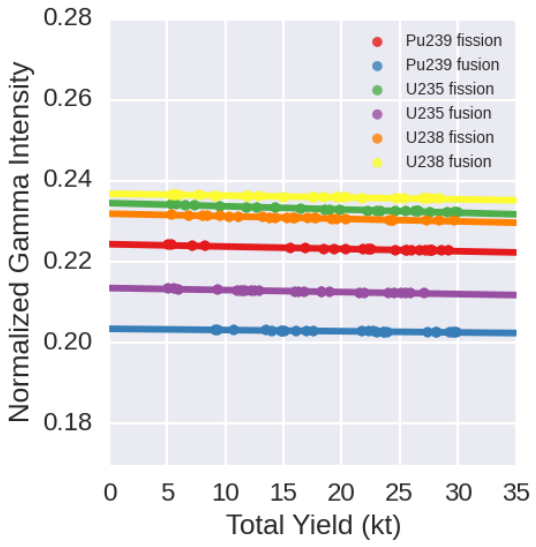

(b)

Linear Regression Results		
No. Observations:	450	
Degrees of freedom Residuals:	438	
Degrees of freedom Model:	11	
R-squared:	1.00	
Model Parameter	**Value**	**Std Error**
β_{0j} intercept parameter :		
239-Pu fission	0.2240	2.15E-05
239-Pu fusion	0.2033	3.14E-05
235-U fission	0.2342	2.83E-05
235-U fusion	0.2133	2.86E-05
238-U fission	0.2316	2.86E-05
238-U fusion	0.2366	2.73E-05
β_{1j} slope parameter :		
239-Pu fission	-4.79E-05	9.57E-07
239-Pu fusion	-2.73E-05	1.43E-06
235-U fission	-7.49E-05	1.29E-06
235-U fusion	-4.55E-05	1.43E-06
238-U fission	-5.39E-05	1.42E-06
238-U fusion	-4.25E-05	1.34E-06

Figure 3-9 Total yield regression results for the 99Mo 140.5 keV line (a) graph of data with regression fit (b) regression table with values of model parameters

Figure 3-9 shows the results from fitting the data. Figure 3-9(a) is the model fit to the data. Figure 3-9(b) is a table of the values for the results. From the table an R-squared value of 1.00 suggests that the linear model 100% explains the variability of the response data around the mean. Another feature of the table is that the normalized gamma intensity does have some dependence on yield since the slope parameters are non-zero. However, what is not evident is

how much fission yield contributes to the variability of the data and whether that change is significant.

To test for significance of total explosive yield, the F-Test was used. For the test the full model was compared to the reduced model where yield parameters (β_{1j}) are assumed to be zero. For the F statistic the hypotheses are:

- Null Hypothesis: $\beta_{1j} = 0$
- Alternate Hypothesis: $\beta_{1j} \neq 0$

We are testing whether the reduced model sufficiently represents the data without considering any slope parameters. The results for the F-test are as follows.

Table 3-5 F-Test results for total yield simulation

DOF Residuals	DOF Difference	SSR Difference	F Value	Pr(>F)
438	6	$2.4 * 10^{-6}$	1076	0.0%

where:

- DOF= Degrees of Freedom
- SSR= sum of squares for residuals
- Pr(> F)= The probability that the F-value will be more extreme than the observed value a.k.a. p-value

From these results we would reject the null hypothesis that total yield parameters are equal to zero. The reason for this is because the p-value is 0%. This is saying that total yield is statistically significant. However, gamma intensity shows a weak dependence on total yield.

3.5 Varying Burst Height

The next parameter examined was burst height. Burst height is expressed in meters above ground level. The low energy, low intensity, and overlapping lines were removed. Below is the complete list of model parameters used in the simulation:

Table 3-6 Parameters used for testing gamma intensity as a function of burst height

Parameters	Simulation Inputs
Fission Type	6 Types： (^{239}Pu, ^{235}U, ^{238}U)x (Fission and Fusion)
Total Yield (kt)	10
Sample locations	3
Burst Height (m)*	Range of 1-100, 25 samples*
Time after blast (d)	5
Particle size (μm)	490-510

* Parameter being analyzed

Table 3-6 shows the model scenarios used for burst height. 25 random burst height values were sampled from a uniform distribution with a minimum of 1 m and maximum of 100 m. A range of 1 to 100 meters was used because underground detonations are beyond the scope of this thesis, and fallout density deposited on the ground is minimal for a 10 kt blast detonated at a burst height greater than 100 meters. The fallout was analyzed at 3 random sites. This was done for every fission type, producing 450 unique gamma spectra to analyze.

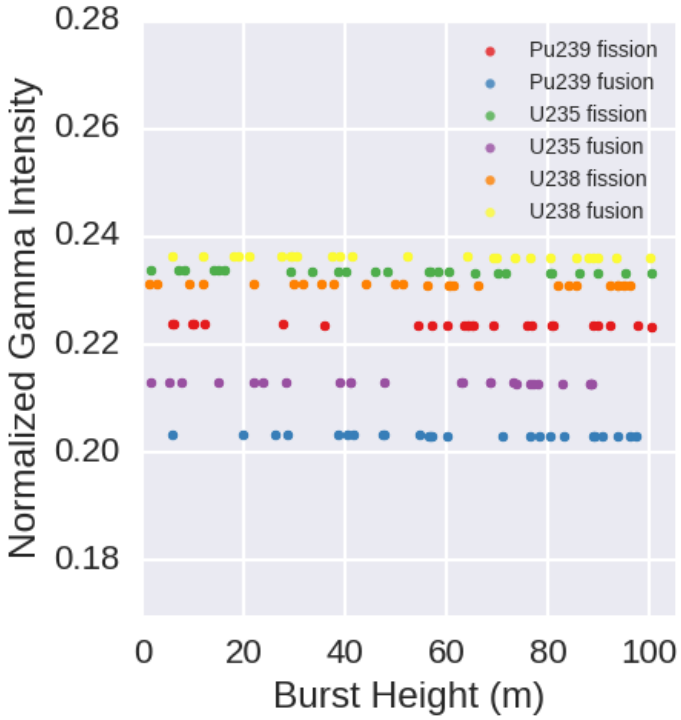

Figure 3-10 Normalized gamma intensity of 140.5 keV (^{99}Mo) as a function of fission type and burst height

Figure 3-10 shows how the gamma intensity changes as burst height varies. From the data it appears that chemical fractionation has a weaker effect on burst height since the distance between the blast and the soil will determine how hot the soil gets, and in turn at what time the soil solidifies. The data also appear to be linear. Last, fission type is the primary distinguishing feature between the differing sets of data.

The same modeling technique was used for both yield and burst height. The primary model variables of interest are the β_{1j} variables, since they model the dependence of normalized gamma intensity on burst height.

(a) **(b)**

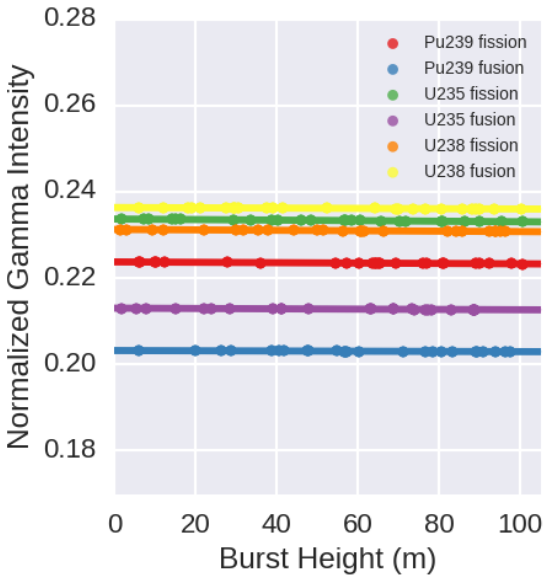

Linear Regression Results	
No. Observations:	450
Degrees of freedom Residuals:	438
Degrees of freedom Model:	11
R-squared:	1.00

Model Parameter	Value	Std Error
β_{0j} intercept parameter :		
239-Pu fission	0.2238	5.87E-07
239-Pu fusion	0.2033	9.08E-07
235-U fission	0.2337	7.96E-07
235-U fusion	0.2131	8.19E-07
238-U fission	0.2313	8.02E-07
238-U fusion	0.2364	8.11E-07
β_{1j} slope parameter :		
239-Pu fission	-4.46E-06	8.97E-09
239-Pu fusion	-2.55E-06	1.38E-08
235-U fission	-6.35E-06	1.28E-08
235-U fusion	-3.72E-06	1.29E-08
238-U fission	-4.98E-06	1.26E-08
238-U fusion	-3.44E-06	1.28E-08

Figure 3-11 Burst height regression results for 140.5 keV, 99Mo (a) graph of data with regression fit (b) regression table with values of model parameters

Figure 3-11(a) and Figure 3-11(b) show the least squares fit of the data. An R-squared value of 1.00 suggests that the linear model 100% explains the variability of the response data around the mean. There are two results to note about the burst height model. The first is that gamma intensity does have some dependence on burst height since the slope parameters are non-zero. The second result to note is the difference in variable magnitude between burst height and total yield from Figure 3-11(a). There is approximately 1 order of magnitude difference between the burst height variables and total yield variable from the previous section (10^{-6} for burst height, 10^{-5} for total yield). The effect is also visible when comparing the graphs; the burst height regression lines have less of a slope. This result shows that soil solidification time does have some dependence on burst height though it is a weaker dependence than it is for total explosive yield.

The same approach F-Test experimental design was used for burst height. For the F-Statistic the hypotheses tested are:

- Null Hypothesis: $\beta_{1j} = 0$
- Alternate Hypothesis: $\beta_{1j} \neq 0$

Table 3-7 F-Test results for burst height simulation

DOF Residuals	DOF Difference	SSR Difference	F Value	Pr(>F)
438	6	$8.0 * 10^{-6}$	235,225	0.0%

Where:

- DOF= Degrees of Freedom
- SSR= sum of squares for residuals
- $\Pr(> F)$= The probability that the F-value will be more extreme than the observed value a.k.a. p-value

From Table 3-7 we would reject the null hypothesis and conclude that burst height is a statically significant parameter. The reason for this is because the p-value is 0%.

3.6 Sensitivity Analysis of Gamma Photo peaks to Fission Type

The previous sections examined the behavior of gamma intensity as a function of various input parameters to a nuclear detonation event. Sample location, total explosive yield, and burst height were each isolated for analysis. The result was that fission type introduced the most variability followed by total yield. For the final analysis, all parameters were varied except for particle size. The statistical analysis and ranking was done using gamma intensity as a function of fission type and total explosive yield. This was done for two reasons: first, total yield and fission type are the largest contributors to variance, and second, total explosive yield can be estimated using techniques other than gamma spectroscopy. One important note is that the results are reported for a specific range of DELFIC input parameters and are not intended to be general conclusion on gamma intensity behavior as a function of all input parameters. Table 3-8 shows the inputs for the final analysis. For consistency, the same sampling ranges and distribution used in the individual parameter analysis were used for the final simulation

Table 3-8 Parameters used for testing gamma intensity while varying multiple input parameters

Parameters	Simulation Inputs
Total Yield (kt)	range of 5-30
Burst Height (m)*	range of 1-100, 25 samples*
Time after blast (d)	3,7,18
Particle size (μm)	490-510

Further tests are needed to see if this holds true for other ranges of DELFIC input parameters. We also analyzed multiple collection times at 3, 7, and 18 days after detonation. Every gamma

line was analyzed and the most active emitter, ^{99}Mo gamma line 140.5 is presented in the subsequent figures.

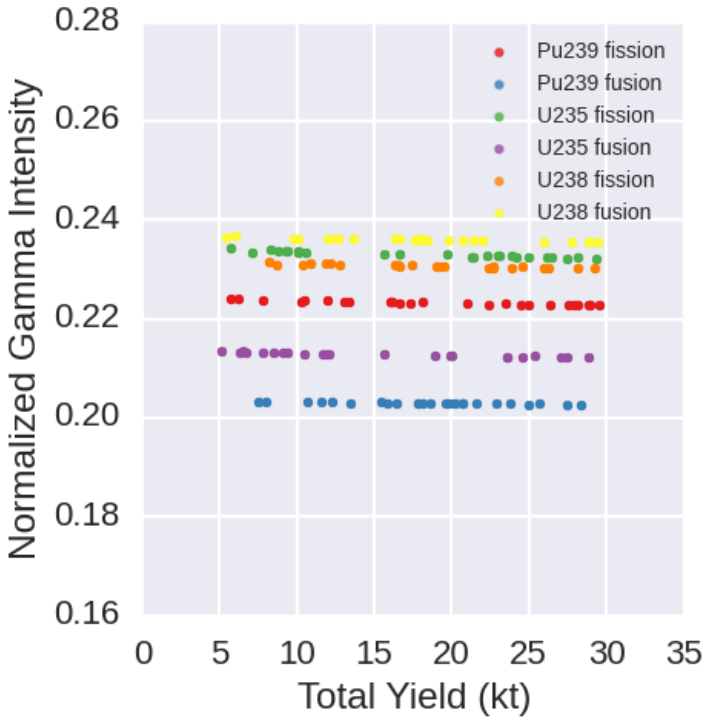

Figure 3-12 Normalized gamma intensity of the ^{99}Mo 140.5 keV line while varying both burst height and total yield

Figure 3-12 shows the results of the final simulation. The figure has all the same features as the explosive yield analysis in Figure 3-8. The data appears linear with slightly more dispersion around the mean then was present in Figure 3-9. Linear regression analysis was then performed on the data. Model equation (2.6) was used to do regression analysis. These are the same equations used for the total explosive yield simulation regression analysis.

Figure 3-13 are the results from the regression analysis. Figure 3-13 (a) is the model fit to the data. Figure 3-13(b) is a table of parameter values with their standard errors. From the table an R-squared value of 1.00 suggests that the linear model 100% explains the variability of the response data around the mean. This result is similar to the result of the total explosive yield analysis. The difference is the increase in standard error for the parameter estimates. The standard error is a measure of the dispersion between the data and the fitted line. It is greater in this simulation due to the introduction of varying burst height. However, they are still extremely small compared to the model values.

(a) **(b)**

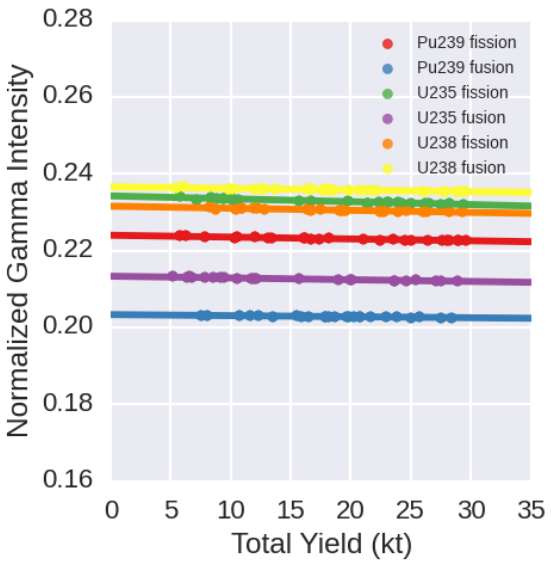

Linear Regression Results		
No. Observations:	441	
Degrees of freedom Residuals:	429	
Degrees of freedom Model:	11	
R-squared:	1.00	
Model Parameter	**Value**	**Std Error**
β_{0j} intercept parameter :		
239-Pu fission	0.2240	3.57E-05
239-Pu fusion	0.2033	5.81E-05
235-U fission	0.2342	4.94E-05
235-U fusion	0.2133	4.72E-05
238-U fission	0.2316	5.46E-05
238-U fusion	0.2366	5.21E-05
β_{1j} slope parameter :		
239-Pu fission	-4.79E-05	1.73E-06
239-Pu fusion	-2.73E-05	2.95E-06
235-U fission	-7.49E-05	2.45E-06
235-U fusion	-4.55E-05	2.47E-06
238-U fission	-5.39E-05	2.75E-06
238-U fusion	-4.25E-05	2.63E-06

Figure 3-13 Final simulation regression results for the ^{99}Mo 140.5 keV line (a) graph of data with regression fit (b) regression table with values of model parameters

Figure 3-14 shows a bar chart of the ^{99}Mo 140.5 keV gamma line intercept parameters with error bars. The error bars smaller than the width of the lines on the top of each bar. The separation between fission types is within the standard error for all 6 fission types. This illustrates how this gamma line could be used to distinguish fission type.

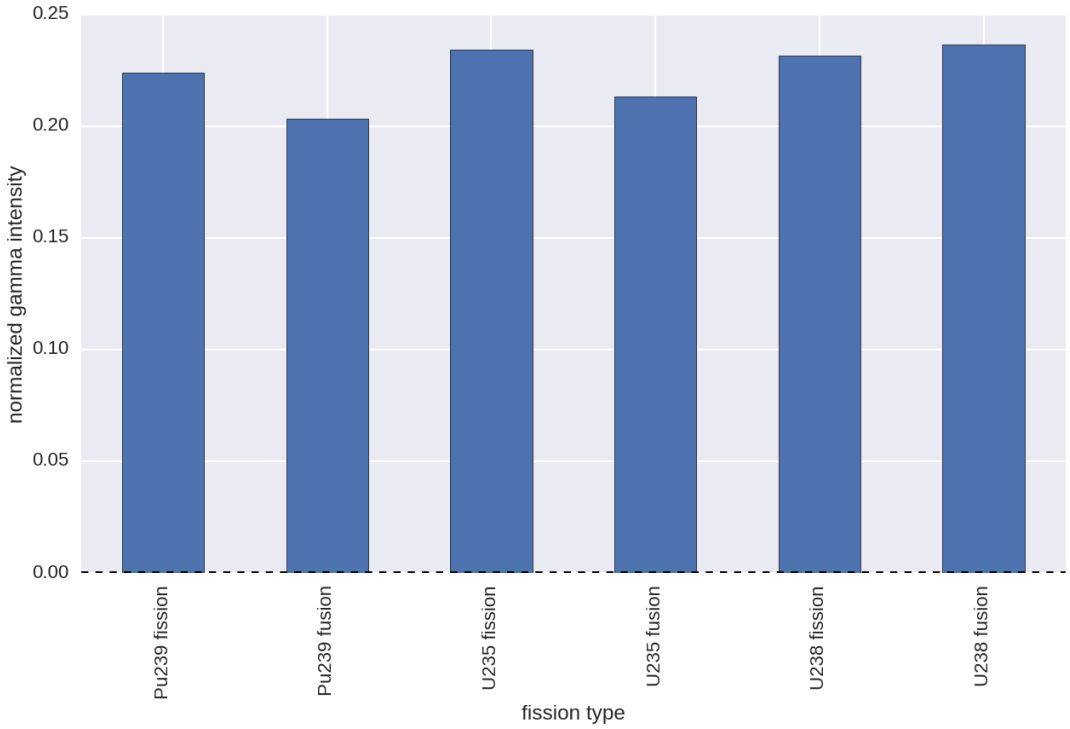

Figure 3-14 Intercept parameters bar chart with error bars for the ^{99}Mo 140.5 keV line

The F-Test was then conducted on the full and reduced models for the final simulation. This was done to determine if fission type is still distinguishable given a known total explosive yield. A value of 10 kt was chosen as a known total yield. The hypotheses tested for the final simulation were:

- Null Hypothesis: $\beta_{0j} = \beta_{0j'}$ for all j, j'

- Alternate Hypothesis: $\beta_{0j} \neq \beta_{0j'}$ for some j, j'

Table 3-9 F-Test results for vary burst height and total yield simulation

DOF Residuals	DOF Difference	SSR Difference	F Value	Pr(>F)
429	5	0.024549	373,928	0.0%

Where:

- DOF= Degrees of Freedom
- SSR= sum of squares for residuals
- Pr(> F)= The probability that the F-value will be more extreme than the observed value a.k.a. p-statistic

From Table 3-9 we would reject the null hypothesis and conclude that the model coefficients are distinguishable given a known total yield of 10 kt. The reason for this is because the p-statistic is 0%.

The final feature analyzed for the normalized gamma intensity of each gamma line was the "separation" between the fission types in the data. The goal of this analysis was to identify which gamma lines are the most useful in distinguishing fission type. Three approaches were used to determine the most useful gamma lines. The first was neutron spectrum only which represent gamma lines that were extremely sensitive to neutron spectrum. The second approach was minimum separation between lines which the distance between each fission type was calculated and the minimum distance was reported. The third approach was standard deviation between the fission types.

For neutron flux only, some gamma lines were extremely sensitive to neutron flux. These gamma lines come from radionuclides that are created in much higher abundance for fission induced by fusion energy neutrons.

Figure 3-15 shows the normalized gamma intensity of two gamma lines that are sensitive to neutron flux. Figure 3-15(a) and (b) show only 3 fission types instead of 6. That is because the gamma intensity from gamma lines 617.4 keV, and 252.4 keV fall below the 10^{-6} normalized intensity threshold for detonations that are induced by fission energy neutrons.

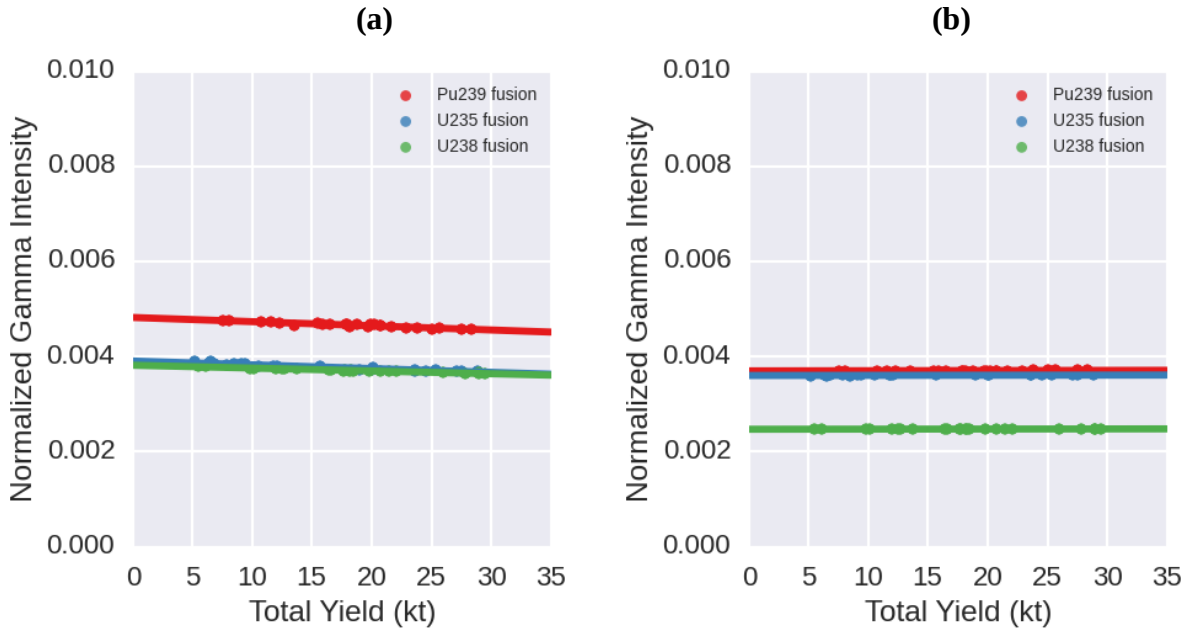

Figure 3-15 Normalized gamma intensity of energy peaks that are sensitive to neutron flux (a) gamma line 617.4. keV from ^{112}Ag (b) gamma line 252.4. keV from ^{127}Sb

Table 3-10 Gamma lines sensitive to neutron spectrum at various collection times

List of gamma lines sensitive to neutron flux Radionuclide, Line Energy(keV)					
3 Days		**7 Days**		**18 Days**	
Sb127	252.4	Sb127	252.4	Sb127	473
Cd115	527.9	In115m	336.24	Ag111	342.13
Ag111	342.13	Ag111	342.13	Sb127	783.6
In115m	336.24	Sb127	445.1		
		Cd115	527.9		
		Sb127	603.5		

Table 3-10 is a list of the gamma lines that are sensitive to neutron flux. One feature to note is that all radionuclides on the list have mass numbers that lie in the "saddle" of the fission product mass yield curve. The next two techniques used to classify the gamma lines were the minimum separation and standard deviation about the mean.

For the final two analysis techniques, the regression model intercept values were used for comparison. For the minimum separation analysis, the distance between each fission type was calculated and the minimum distance was reported. The rankings reflect the gamma lines with the largest minimum separation aka the maximum minimum. Standard deviation about the mean was straight-forward. The standard deviation of the data was reported and ranked by the radionuclides with the largest standard deviation.

Table 3-11 Ranking of gamma lines with the greatest standard deviation between Fission Type model parameters at various collection times

Standard deviation Between Fission Type Radionuclide, Line Energy(keV), Standard Deviation									
Rank	**3 Days**			**7 Days**			**18 Days**		
1	Rh105	318.9	9.028E-03	La140	1596.2	1.035E-02	Ru103	497.1	2.122E-02
2	Ce143	293.3	7.944E-03	Ru103	497.1	9.659E-03	La140	1596.2	9.220E-03
3	Zr97	743.4	7.537E-03	I131	364.5	7.470E-03	I131	364.5	8.614E-03
4	Mo99	140.5	5.718E-03	Mo99	140.5	6.395E-03	Zr95	756.7	8.313E-03
5	Te132	228.2	5.138E-03	Te132	228.2	6.269E-03	Nb95	765.8	5.079E-03
6	Ag112	617.4	4.658E-03	Sb127	685.7	5.648E-03	Cs136	818.5	4.868E-03
7	Nb97	657.9	4.290E-03	La140	487.0	4.930E-03	Ce141	145.4	4.550E-03
8	Sb127	685.7	4.171E-03	Sb127	473.0	3.962E-03	La140	487.0	4.393E-03
9	La140	1596.2	3.688E-03	Xe133	81.0	3.782E-03	Nd147	91.1	3.924E-03
10	Ru103	497.1	3.661E-03	Cs136	818.5	3.362E-03	Cs136	1048.1	3.912E-03
11	Sb127	473.0	3.095E-03	Ce141	145.4	3.113E-03	Xe133	81.0	2.396E-03
12	I131	364.5	3.046E-03	I132	772.6	2.884E-03	Mo99	140.5	2.304E-03
13	In115m	336.2	2.439E-03	Ce143	293.3	2.867E-03	Sb126	414.7	2.280E-03
14	Ce143	57.4	2.170E-03	Cs136	1048.1	2.700E-03	La140	815.8	2.249E-03
15	Xe133	81.0	2.022E-03	Zr95	756.7	2.613E-03	Sb127	685.7	2.234E-03

Table 3-12 Ranking of gamma lines with the maximum separation between Fission Type model parameters at various collection times

Maximum Minimum Between Fission Type Radionuclide, Line Energy(keV), Minimum Separation									
Rank	**3 Days**			**7 Days**			**18 Days**		
1	Ru103	610.3	0.000492	In115m	336.2	3.00E-07	Zr95	724.2	8.19E-07
2	Na24	2754.0	2.00E-05	La140	1596.2	2.78E-07	La140	1596.2	5.50E-07
3	I132	772.6	6.50E-07	Ba140	304.9	2.39E-07	Ru103	497.1	3.81E-07
4	Ce143	293.3	4.06E-07	Ru103	497.1	1.89E-07	La140	487.0	2.62E-07
5	In115m	336.2	3.93E-07	Ce141	145.4	1.72E-07	Ru103	557.1	2.47E-07
6	Cd115	527.9	2.16E-07	Cd115	527.9	1.65E-07	Ce141	145.4	2.06E-07
7	Rh105	318.9	1.47E-07	La140	487.0	1.33E-07	La140	815.8	1.34E-07
8	La140	1596.2	1.28E-07	Ag112	617.4	1.17E-07	Ba140	537.3	1.22E-07
9	Ag112	617.4	1.25E-07	Cd115	492.4	9.47E-08	La140	328.8	1.17E-07
10	Mo99	140.5	1.23E-07	Mo99	140.5	9.25E-08	La140	925.2	3.98E-08
11	Ag112	1387.7	1.18E-07	La140	815.8	6.80E-08	Ag111	342.1	3.53E-08
12	Ce143	57.4	1.11E-07	Ba140	537.3	6.30E-08	La140	867.9	3.17E-08
13	Cd115	492.4	1.09E-07	La140	328.8	5.93E-08	Ba140	162.7	3.12E-08
14	Ce143	664.6	8.59E-08	Cs136	818.5	4.29E-08	Cs136	1235.4	2.91E-08
15	Cs136	818.5	7.77E-08	Cs136	1048.1	3.45E-08	Zr95	756.7	2.53E-08

Table 3-11 and Table 3-12 are the final result for this analysis. They show a ranking of which radionuclides are useful in distinguishing fission type. These results are consistent with the fission mass yield curve, as many of the radionuclides with high rankings are location on the edges of the fission mass yield curves or in the saddle. Those ranges are mass chains in the 95-105 range and some in the 140-145 range for the edges and 110-136 for the saddle.

(a) **(b)**

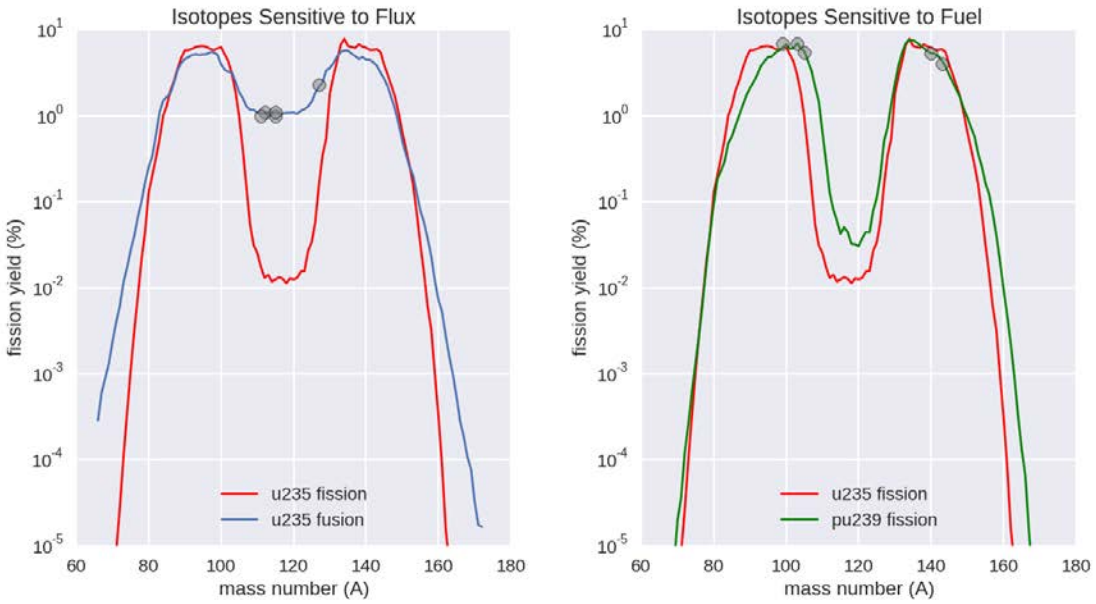

Figure 3-16 Highest ranking radionuclides for distinguishing fission type (a) radionuclides sensitive to neutron flux (b) radionuclides sensitive to fissile fuel material

Figure 3-16 are plots of the highest ranking radionuclides and their location on the fission mass yield curve. Figure 3-16(a) depicts the radionuclides most sensitive to neutron flux, while Figure 3-16(b) depicts the radionuclides most sensitive to fissile fuel material.

4 Conclusions/Future Work

The goal of this thesis was to develop a method that could identify characteristics of nuclear devices faster than chemical analysis by measuring the gamma spectrum of the radioactive daughter products contained in fallout particles after the detonation. This work showed that controlling particle size of the fallout particles greatly reduced the variance in radionuclide inventory, and hence gamma spectrum, of fallout particles. The reduction in variance was so significant that fuel type and neutron flux often become the only distinguishing feature for several mass chains. The mass chains that show a distinction between fuel type and neutron energy spectrum were consistent with well-established fission mass yield curve data. Mass chains located in the saddle of the mass yield curve were sensitive to neutron flux. Mass chains sensitive to fuel type were located on the edges of the mass yield curve. This information is useful in that it would allow nuclear forensics experts the ability to identify characteristics about nuclear devices by conducting gamma spectroscopy on site as soon as they arrive.

The primary mechanism for this variance reduction was achieved by controlling particle size, which reduced the effects of physical fractionation. The idea explored was that when fallout particles are sampled in bulk, particles with the same surface to volume ratio (same particle diameter) have the same abundance of volatile and refractory mass chains contained in the particles. This was tested by running DELFIC simulations, where normalized gamma spectrum was treated as a dependent variable of various DELFIC input parameters and observation conditions. The results of each simulation were then modeled using linear regression. Linear modeling was possible, if and only if, particle size is controlled.

Another result of this work demonstrated how chemical fractionation affects the gamma spectrum. This was tested by varying burst height and total explosive yield. Varying these input parameters changed the soil solidification time and hence the degree of chemical fractionation of

some mass chains. The result is that gamma spectrum of a single particle diameter exhibits a very small dependence on total explosive yield and burst height. The F-Test was then conducted for each input parameter to statistically quantify the importance of explosive yield and burst height. The result was that both input parameters are statistically significant. However, distinguishing fuel material and neutron flux was still possible when both explosive yield and burst height were varied. Furthermore, burst height and total explosive yield can be estimated by other means then gamma spectroscopy (crater size and/or height of mushroom cloud, for example).

The potential for using gamma spectroscopy for prompt nuclear forensics is a promising field which could allow experts to identify device characteristics sooner when compared to other nuclear forensics techniques. However, the accuracy of making determinations about device characteristics based on nuclear fallout is highly dependent on the degree of fractionation present in the fallout being measured. This work showed that controlling particle size is one technique that can be effective in reducing the effect of physical fractionation. Combining this technique with prior work and future analysis methods could prove useful in making more accurate determinations of nuclear device characteristics.

4.1 Future Work/Recommendations

- This work only explored particles sizes of 490-510 μm. This is a relatively large particle size and would reflect primarily refractory radionuclides. The same analysis could be conducted on different particles sizes to determine if the behavior is consistent for all particles sizes.
- A 20 μm range (490-510) was the only range tested in this work. This represented a single particle size bin in DELFIC. Future work on larger ranges of particles sizes could also be conducted. Determination of the range of particle sizes at which linear modeling no longer becomes feasible could be explored.

- Homogenous fuel material and single neutron flux per device were the inputs that were tested. Future work could be conducted on analyzing the spectrum from devices composed of mixed fuel and multiple neutron fluxes.
- This analysis was based on computer simulations, and hence, the validity of the results is highly dependent on how well the models used in DELFIC reflect physical reality, namely fractionation. Any future work that compares the results found in this paper to results achieved by other nuclear fallout simulation codes and fractionation models would be useful.
- Different statistical treatment of the data could also be used. Bayesian analysis for example could be used to determine the probability of a device being made from a specific fuel material and neutron energy given the observed gamma spectrum.

5 Works Cited

[1] B. Obama, "National Security Strategy," 2015.

[2] W. Dunlop and H. Smith, "Who did it? Using International Forensics to Detect and Deter Nuclear Terrorist," *Arms Control Today*, vol. 36, no. 8, p. 6, 2006.

[3] D. Hooper and R. L. M. M. Vincent Jodoin, "Predictive Fallout Composition Modeling: Improvements and Applications of the Defense Land Fallout Interpretive Code," in *INMM Paper*, Orlando, Florida, 2012.

[4] R. Heft, "the Characterization of Radioactive Particles from Nuclear Weapons Tests," *Advances in Chemistry: American Chemical Society*, vol. 7, no. 2, pp. 254-281, 1970.

[5] E. Freiling, "Radionuclide Fractionation in Bomb Debris," *Science, New Series*, vol. 133, no. 3469, pp. 1991-1998, 1961.

[6] S. Freiling and E. Rainey, "Fractionation II. On Defining the Surface Density of Contamination," U.S. Naval Radiological Defense Laboratory. USNRDL-TR-931, San Francisco, CA, 1963.

[7] H. Miley, R. Arthur, E. Lepel, S. Pratt and C. Thomas, "Evaluation of fission product isotopes for field or labortory detection," *Journal of Radioanalytical and Nuclear Chemistry*, vol. 248, no. 3, pp. 651-656, 2001.

[8] R. Marrs, E. Norman, J. Burke, R. Macri, H. Shugart, E. Browne and A. Smith, "Fission-product gamma-ray line pairs sensitive to fissile material and neutronenergy," *Nuclear Instruments and Methods in Physics Research A*, vol. 592, pp. 463-471, 2008.

[9] T. Miller, "Early Time Characterzation of Fresh Nuclear Debris Using Gamma Spectroscopy," Phd Dissertation. AFIT/DS/ENP/10-S04. School of Engineering, Air Force Institute of Technology, Wright Patterson Air Force Base, OH, 2010.

[10] B. Smith, "Near-Time Characterization of a Domestic Nuclear Event Using Gamma Spectroscopy," MS Thesis. AFIT/GNE/ENP/08-M06. School of Engineering, Air Force Institute of Technology, Wright Patterson Air Force Base, Ohio, 2008.

[11] H. Norment, "DELFIC Volume I - Fundamentals," Washington D.C., 1979.

[12] H. Norment, "DELFIC: Department of Defense Fallout Prediction System: Volume II users manual," Defense Nulcear Agency, Washington D.C., 1979.

[13] Oak Ridge National Laboratories, "SCALE Overview," Sep 2004. [Online]. Available: http://scale.ornl.gov/overview/origens.htm. [Accessed Feb 2016].

[14] S. Glasstone and P. Dolan, The Effects of Nuclear Weapons, Department of Defense and

Department of Energy, 1977.

[15] ORNL, "ORIGEN-S Data Libraries, TM-2005/39 Version 6.1 Sect. M6," Radiation Information Computational Center, 2005.

[16] A. Nichols, D. Aldama and M. Verpelli, Handbook of Nuclear Data for Safeguards: Database Extension, August 2008, Vienna, Austria: International Atomic Energy Agency, 2008.

[17] Y. A. Izrael, Radioactive Fallout After Nuclear Explosions and Accidents, Kidlington, Oxford UK: Elsevier Science Ltd. , 2002.

[18] G. Knoll, Radiation Detection and Measurement 4th ed., Ann Arbor, MI: John Wiley and Sons, Inc., 2010.

[19] C. Svensson and G. Hackman, "Position sensitivity of the TIGRESS 32-fold segmented HPGe clover detector," *Nuclear Instruments and Methods in Physics Research A*, vol. 540, pp. 348-360, 2005.

[20] E. Freiling, M. Kay and J. Sanderson, "Fractionation IV. Illustrative Calculations of The Effect of Radionuclide Factionation on Exposure-Dose Rate from Local Fallout," USNRDL-TR-715, U.S. Naval Radiological Laboratory , San Fransico, California, 1964.

[21] D. Morris, "A predictive technique for forecasting the isotopic composition of radioactive fallout," Phd Dissertation. AFIT/DS/ENP/04-02, AD B3040511. School of Engineerin, Air Force Institute of Technology, Wright-Patterson AFB OH, 2004.

[22] E. Freiling, "Fractionation III. Estimation of Degree of Fractionation and Radionuclide Partition for Nuclear Debris," *Naval Radiological Defense Laboratory* , Vols. USNRDL-TR-680, 1963.